User-Pair Scheduling and Mode Selection in Asymmetric Full-Duplex Systems With Limited Feedback: Algorithm and Scaling Laws

Rama Kiran and Neelesh B. Mehta, *Fellow, IEEE*

***Abstract*— Determining which users to simultaneously schedule on the uplink and the downlink in a full-duplex (FD) system is crucial to control the inter-user interference between them and achieve a high spectral efficiency. The user-pair scheduling algorithm and the efficacy of FD is, thus, closely linked to the availability of channel state information and the feedback scheme that conveys it to the base station (BS). We consider a reduced feedback scheme in which a user that is scheduled feeds back only a limited number of quantized inter-user interferences that are below a pre-specified threshold. For it, we propose a novel user-pair scheduling and mode selection algorithm (UPSMA). We analyze the uplink and downlink spectral efficiencies of UPSMA for two channel models that highlight the different influences of small-scale fading and large-scale shadowing. We derive insightful asymptotic scaling laws that quantify the dependence of the threshold and the uplink and downlink spectral efficiencies on the number of users. UPSMA with limited feedback achieves a higher sum spectral efficiency than a half-duplex system and conventional FD resource allocation algorithms. Its performance is close to the exhaustive search algorithm in which the BS knows all the inter-user interferences.**

***Index Terms*— Cellular communications, full-duplex communications, user scheduling, feedback, mode selection.**

I. Introduction

A FULL-DUPLEX (FD) base station (BS) can simultaneously transmit and receive signals on the same frequency band. Consequently, FD has the potential to increase the spectral efficiency of next generation cellular systems. However, several new challenges arise in the implementation of FD. The first challenge is the self-interference (SI) at the BS, which is caused by power leakage from its transmitter to its receiver. Software and hardware techniques, such as analog and digital domain subtractions of the transmitted signal from the received signal and transmit precoding have been proposed to reduce SI. Their practical feasibility has also been demonstrated [2].

The second challenge is the interference from the user that transmits on the uplink to the user that receives on the downlink. In order to mitigate this inter-user interference, the BS needs to carefully choose the uplink and downlink users or revert to the conventional half-duplex (HD) mode. User scheduling and mode selection are intimately linked to the availability of information about inter-user interference at the BS, since it affects the downlink signal-to-interference-plus-noise ratio (SINR) in an FD system. This, in turn, depends on the feedback scheme. The literature, which we summarize below, differs considerably on its assumptions about channel state information (CSI) and feedback, and the criteria used to schedule the users.

A. Scheduling and Mode Selection in FD Cellular Systems

In [3]–[5], the BS schedules the uplink and downlink users that are sufficiently spaced apart to mitigate the inter-user interference. In [6], the BS is assumed to know the distance between any two users in the cell but not their inter-user interferences. For each downlink user, it pairs an uplink user that is farthest away from it. It reverts to the HD mode if the probability that their inter-user interference less than a threshold falls below a minimum value. Three algorithms that schedule the uplink and downlink users are analyzed by Alexandropoulos, Kantouris, and Atzeni (AKA) in [7]. In the first algorithm AKA-1, the BS selects the uplink and downlink users with the largest channel gains. In the second algorithm AKA-2, the BS first selects the uplink user with the largest channel gain. It then selects the downlink user with the largest SINR assuming that the BS knows the gains of all the inter-user channels involving the uplink user. The third algorithm AKA-3 is similar to AKA-2 except that the downlink user is selected first and the uplink user next. Asymptotic scaling laws for the sum throughput are derived for these algorithms. A scheduling algorithm is proposed in [8] that maximizes the system throughput while ensuring a minimum throughput for each user. Given a downlink user, the algorithm in [9] pairs with it the user that maximizes the sum of the uplink and downlink rates or minimizes the sum of outage probabilities of the uplink and the downlink. All

Manuscript received June 6, 2020; revised October 19, 2020; accepted December 6, 2020. Date of publication December 22, 2020; date of current version May 10, 2021. This work was supported in part by the Visvesvaraya Ph.D. Scheme for Electronics and IT, the Indigenous 5G Test Bed Project of the Department of Telecommunications, India, and in part by the Department of Science and Technology (DST)-Swaranajayanti Fellowship under Award DST/SJF/ETA-01/2014-15. This article was presented at the 2020 IEEE Global Communications Conference (IEEE GLOBECOM). The associate editor coordinating the review of this article and approving it for publication was J. Yuan. *(Corresponding author: Neelesh B. Mehta.)*

The authors are with the Department of Electrical Communication Engineering (ECE), Indian Institute of Science (IISc), Bengaluru 560012, India (e-mail: ramakiranab@gmail.com; neeleshbmehta@gmail.com).

Color versions of one or more figures in this article are available at https://doi.org/10.1109/TWC.2020.3044919.

Digital Object Identifier 10.1109/TWC.2020.3044919

the above papers assume a time division duplexing (TDD) system.

FD for orthogonal frequency division multiple access (OFDMA) is considered in [10]–[27]. In [10], for each sub-carrier, the BS schedules an uplink user with the largest uplink channel gain and the downlink user with the highest downlink SINR among the other users. In [11], the user pairing and subchannel allocation problem is modeled as a three-sided matching game, for which a stable matching algorithm is proposed. Similarly, [12] models user pairing in a femto-cell network as a two-sided game. In [13], the user-pair with the highest sum spectral efficiency whose inter-user interference is less than a threshold is scheduled on a subcarrier. In [14], uplink and downlink users are paired using the Hungarian method to maximize the sum spectral efficiency. In [15], a scheme based on auction and matching theories is proposed. It guarantees that the users report true values of their channel quality and utilities.

In [16], a heuristic algorithm is proposed to maximize the sum rate when the BS knows only the inter-user distances and the distances between the BS and the users. In [17], a two-part approach that uses fast-Lipschitz optimization for determining the transmit powers and a greedy algorithm to pair users and assign them to the subcarriers is proposed. In [18], a multi-objective optimization problem is formulated to study the interplay between weighted sum spectral efficiency maximization and fairness. Fairness is also accounted for in [19]–[21]. Iterative sub-carrier allocation algorithms that maximize the sum throughput subject to power constraints at the BS and users are proposed in [22]–[25]. In [26], the BS uses an evolutionary algorithm to schedule users. FD and non-orthogonal multiple access are considered together in [27].

Comments: In [25], [26], inter-user interference is not considered for scheduling. The algorithms that are based on user separation in [3]–[6], [16] do not consider the effect of small-scale fading and shadowing on the inter-user interference. In [8], [9], [11], [13], [14], [17]–[24], [27], the BS is assumed to know the inter-user channel gains of all the user-pairs in the cell. This is practically challenging since the BS cannot estimate an inter-user channel gain by itself; it needs them to be fed back. Since there are $\binom{N}{2}$ user-pairs in a cell with N users, the feedback overhead grows as N^2 and can overwhelm the uplink. The algorithms in [12], [15] also require a similar number of exchanges of information among the users. The algorithms in [7], [10] reduce the number of inter-user channel gains that the BS needs to know to $N-1$, but assume that this information is available to the BS with infinite resolution.

B. Contributions

We propose a novel user-pair scheduling and mode selection algorithm (UPSMA) and a reduced inter-user interference feedback scheme for a cellular system with an FD-capable BS and HD users. We focus on this asymmetrical model because FD is likely to be first implemented in the BS transceiver than in handsets because of the advanced hardware and software algorithms it requires. We make the following contributions:

1) *Scheduling, Mode Selection, and Feedback:* In UPSMA, the BS first schedules a user on either the uplink or the downlink. The scheduled user feeds back a set containing at most L users and b-bit quantized versions of the inter-user interferences from them. Here, L and b are system parameters that control the feedback overhead. Only users whose inter-user interference are less than a threshold γ_{th} can be included in the set. The threshold γ_{th} is a system parameter that is optimized to maximize the spectral efficiency. This also enables the BS to bound the inter-user interference and conservatively estimate the downlink SINR before it determines which users to pair. The BS schedules the second user from among the users that are fed back. The BS can also revert to the HD mode if it has a higher spectral efficiency or the feedback set is empty.
2) *Spectral Efficiency Analysis:* We derive expressions for the uplink and downlink spectral efficiencies of UPSMA in a single-cell scenario for the general case in which the channels between the users and the BS are statistically non-identical and so are the inter-user interferences. This analysis is more involved and is considerably different from that of an HD system because of the inter-user interference and the limited feedback about it, which itself depends on the user that is scheduled first.
3) *Asymptotic Analysis:* We derive insightful asymptotic scaling laws that quantify how the optimal γ_{th}, which maximizes the sum spectral efficiency, and the uplink and downlink spectral efficiencies depend on the number of users and the feedback set size. We do this for two common channel models: i) Fading-pathloss model, in which the channels undergo small-scale fading and pathloss [7], [9], [12]. ii) Fading-shadowing-pathloss model, in which the channels undergo small-scale fading, large-scale shadowing, and pathloss. The latter model is more realistic but has received less attention in the FD literature. These laws turn out to be very different for the two models, and highlight the different impacts of small-scale fading and large-scale shadowing on the spectral efficiency of FD cellular systems. They are different from the laws derived in [7], which assumed the availability of CSI with infinite resolution and focused only on the fading-pathloss model. They also differ from the corresponding laws for HD systems due to inter-user interference and the new system design aspects introduced by the limited feedback set.
4) *Simulation Results and Benchmarking:* We present extensive simulation results to benchmark the spectral efficiency gains from UPSMA in the noise-limited single-cell scenario and the co-channel interference-limited multi-cell scenario with imperfect SI suppression. These bring out the critical role that feedback plays in an FD system.

C. Outline and Notation

The paper is organized as follows. Section II describes the system model. UPSMA is presented in Section III and its

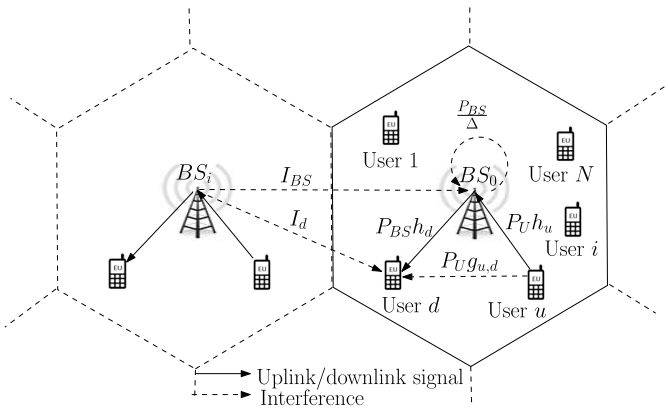

Fig. 1. System model illustrating uplink and downlink channels, inter-user interference, SI and co-channel interference from the neighboring cells.

performance is analyzed in Section IV. Simulation results are presented in Section V, and are followed by our conclusions in Section VI.

Notation: The probability of an event A is denoted by $\mathbb{P}(A)$ and the conditional probability A given B is denoted by $\mathbb{P}(A|B)$. The probability density function (PDF) and cumulative distribution function (CDF) of a random variable (RV) X are denoted by $f_X(\cdot)$ and $F_X(\cdot)$, respectively. $X_n \xrightarrow{d} X$ denotes convergence in distribution of the sequence of RVs $X_1, X_2, \ldots$ to the RV X. The expectation over an RV X is denoted by $\mathbb{E}_X[\cdot]$ and the expectation conditioned on an event A is denoted by $\mathbb{E}_X[\cdot|A]$; the subscript is dropped when it is obvious from the context. And, $X \sim \mathcal{N}(0, \sigma^2)$ means that X is a real Gaussian RV with zero mean and variance σ^2. The cardinality of a set $\mathcal{A}$ is denoted by $|\mathcal{A}|$ and the empty set by $\emptyset$. The set difference between sets $\mathcal{A}$ and $\mathcal{B}$ is denoted by $\mathcal{A} \setminus \mathcal{B}$. The indicator function is denoted by $1_{\{a\}}$; it is 1 if a is true and is 0 otherwise. The Gaussian Q-function [28, Ch. 26.2] is denoted by $Q(\cdot)$ and the Euler-Mascheroni constant [28, Ch. 6.1] by E. We use $O(\cdot)$ and $\Theta(\cdot)$ as per the Bachmann-Landau notation [29, Ch. 2.2].

II. System Model

We consider a cellular system with an FD-capable BS and N HD users per cell. It operates in the TDD mode [3]–[9]. Let $\mathbb{N} = \{1, 2, \ldots, N\}$ be the set of indices of the users. Let the channel power gain between user $m \in \mathbb{N}$ and the BS be denoted by h_m. And, let the channel power gain between users m and n be $g_{m,n}$. For brevity, we call them as channel gains henceforth. The system model is illustrated in Fig. 1. Every user has data to transmit to the BS on the uplink and receive from it on the downlink. We consider the following two channel models:

- *Fading-Pathloss Model:* In this model,

$$h_m = \alpha_m \mu_m, \tag{1}$$

where α_m is a exponential RV with unit mean that models small-scale fading and $\mu_m = K\left(d_0/d_m\right)^\eta$ is the pathloss between the BS and user m. Here, d_m is the distance between the BS and user m, d_0 is the critical distance, K is a constant, and η is the pathloss exponent. Similarly, $g_{m,n} = \alpha_{m,n}\mu_{m,n}$, where $\alpha_{m,n}$ is a exponential RV with unit mean, $\mu_{m,n} = K\left(d_0/d_{m,n}\right)^\eta$, and $d_{m,n}$ is the distance between users m and n.

- *Fading-Shadowing-Pathloss Model:* In this model,

$$h_m = \alpha_m \beta_m \mu_m, \tag{2}$$

where α_m and μ_m are as described above and β_m models shadowing. It is a lognormal RV with dB-mean 0 and dB-standard deviation σ_{dB}. Similarly, $g_{m,n} = \alpha_{m,n}\beta_{m,n}\mu_{m,n}$, where $\beta_{m,n}$ is a lognormal RV with dB-mean 0 and dB-standard deviation σ_{dB}.

SINR Expressions: The received SINRs at the BS and the users are as follows.

1) FD Mode: In the asymmetric model, the FD BS receives a signal from an HD user u and transmits to an HD user $d \neq u$ simultaneously. Therefore, the FD mode uplink SINR $\gamma_{\text{UL}}^{\text{FD}}(u)$ is given by

$$\gamma_{\text{UL}}^{\text{FD}}(u) = \frac{P_{\text{U}} h_u}{\frac{P_{\text{BS}}}{\Delta} + I_{\text{BS}} + \sigma_{\text{ul}}^2}, \tag{3}$$

where P_{U} and P_{BS} are the transmit powers of the users and the BS, respectively, I_{BS} is the co-channel interference power from the neighboring cells at the BS, σ_{ul}^2 is the noise power, and Δ is the SI suppression factor that leads to a residual SI of P_{BS}/Δ. Similarly, the FD mode downlink SINR $\gamma_{\text{DL}}^{\text{FD}}(u, d)$ is given by

$$\gamma_{\text{DL}}^{\text{FD}}(u, d) = \frac{P_{\text{BS}} h_d}{P_{\text{U}} g_{u,d} + I_d + \sigma_{\text{dl}}^2}, \tag{4}$$

where I_d is the co-channel interference power from the neighboring cells and σ_{dl}^2 is the noise power at the users.

2) HD Mode: The BS either receives a signal from a user u or it transmits a signal to a user d, where $u, d \in \mathbb{N}$. When the BS receives, the HD mode uplink SINR $\gamma_{\text{UL}}^{\text{HD}}(u)$ is given by

$$\gamma_{\text{UL}}^{\text{HD}}(u) = \frac{P_{\text{U}} h_u}{I_{\text{BS}} + \sigma_{\text{ul}}^2}. \tag{5}$$

When the BS transmits, the HD mode downlink SINR $\gamma_{\text{DL}}^{\text{HD}}(d)$ is given by

$$\gamma_{\text{DL}}^{\text{HD}}(d) = \frac{P_{\text{BS}} h_d}{I_d + \sigma_{\text{dl}}^2}. \tag{6}$$

CSI Model: We assume that the BS knows the channel gains $h_1, h_2, \ldots, h_N$. It can estimate them from the uplink pilots since the system operates in the TDD mode. We also assume that a BS knows $\left(I_i + \sigma_{\text{dl}}^2\right)$, $\forall i \in \mathbb{N}$. This can be achieved by each user periodically measuring and feeding back its co-channel interference plus noise power to the BS. Only a user knows the inter-user interference between it and the other users in the cell, not the BS.

III. UPSMA

We first present the inter-user interference feedback scheme and then UPSMA.

A. Inter-User Interference Feedback Scheme

Let the BS select a user f for feedback, which can be an uplink or a downlink user. The criterion for selection is described next in Section III-B. The selected user feeds back a set $\mathcal{B}_f$ that contains at most L users and b-bit quantized versions of the inter-user interferences from them. Only users whose interferences lie below a threshold γ_{th} can be included in the set. If there are more than L such users, then the users with the L lowest interferences are fed back. The inter-user interference is quantized as follows. For $b = 1$ bit, the two quantization levels are γ_{th} and γ_{th}/G, where G is a system parameter. For $b = 2$ bits, the four quantization levels are γ_{th}, γ_{th}/G, γ_{th}/G^2, and γ_{th}/G^3, and so on. This ensures that the quantization levels are equi-spaced in dB scale. For *index-only feedback*, i.e., $b = 0$, user f only feeds back the indices of the users.

B. Description of UPSMA

UPSMA schedules the uplink and downlink users in a slot in two steps.

1) Scheduling the First User f: From the CSI available to it, it can be seen from (3) that the BS can compute the uplink SINR. However, this is not the case for the downlink SINR $\gamma_{\text{DL}}^{\text{FD}}(u,d)$ in (4) because the inter-user interference depends on the uplink user that it is yet to choose. Even so, the BS can conservatively estimate $\gamma_{\text{DL}}^{\text{FD}}(u,d)$ using γ_{th} as follows. Since only inter-user interferences that are below γ_{th} are fed back, it follows that

$$\gamma_{\text{DL}}^{\text{FD}}(u,d) \geq \hat{\gamma}_{\text{DL}}^{\text{FD}}(d) \triangleq \frac{P_{\text{BS}} h_d}{\gamma_{\text{th}} + I_d + \sigma_{\text{dl}}^2}, \quad \forall u \in \mathcal{B}_f. \tag{7}$$

We shall refer to $\hat{\gamma}_{\text{DL}}^{\text{FD}}(d)$ as the *conservative FD mode downlink SINR*.

Let $\gamma_{\text{UL}}^* = \max_{i\in\mathbb{N}} \{\gamma_{\text{UL}}^{\text{FD}}(i)\}$ and $\gamma_{\text{DL}}^* = \max_{i\in\mathbb{N}} \{\hat{\gamma}_{\text{DL}}^{\text{FD}}(i)\}$. If $\gamma_{\text{UL}}^* \geq \gamma_{\text{DL}}^*$, then the uplink user $f = \text{argmax}_{i\in\mathbb{N}} \{\gamma_{\text{UL}}^{\text{FD}}(i)\}$ is selected. Else, the downlink user $f = \text{argmax}_{i\in\mathbb{N}} \{\hat{\gamma}_{\text{DL}}^{\text{FD}}(i)\}$ is selected. The selected user f then feeds back the set $\mathcal{B}_f$ to the BS, as described in Section III-A.

2) Scheduling the Second User s: If $\mathcal{B}_f = \emptyset$, the BS skips this step. Else, there are two possibilities that depend on f:

- *f is an Uplink User:* The BS selects the user $s \in \mathcal{B}_f$ for the downlink that maximizes the sum of the uplink and downlink spectral efficiencies as follows:

$$s = \underset{i\in\mathcal{B}_f}{\text{argmax}} \{\log_2\left(1+\gamma_{\text{UL}}^{\text{FD}}(f)\right) + \log_2\left(1+\gamma_{\text{DL}}^{\text{FD}}(f,i)\right)\}. \tag{8}$$

  At this stage, the BS can compute the FD mode downlink SINR $\gamma_{\text{DL}}^{\text{FD}}(f,i)$ more precisely if $b \geq 1$. Specifically, it uses the upper limit of the quantization interval in which inter-user interference lies to calculate $\gamma_{\text{DL}}^{\text{FD}}(f,i)$ instead of the larger γ_{th}, which is used in (7). This leads to a higher SINR than $\hat{\gamma}_{\text{DL}}^{\text{FD}}(i)$. For $b = 0$ bits, it continues to use the conservative estimate $\hat{\gamma}_{\text{DL}}^{\text{FD}}(i)$ of (7) as it has no additional information about the inter-user interference.
- *f is a Downlink User:* The BS schedules the user s for the uplink that maximizes the sum spectral efficiency as follows:

$$s = \underset{i\in\mathcal{B}_f}{\text{argmax}} \{\log_2\left(1+\gamma_{\text{UL}}^{\text{FD}}(i)\right) + \log_2\left(1+\gamma_{\text{DL}}^{\text{FD}}(i,f)\right)\}. \tag{9}$$

3) Mode Selection: The BS selects the HD mode if $\mathcal{B}_f = \emptyset$ or the FD mode sum spectral efficiency is less than the HD mode spectral efficiency of the user $f' = \text{argmax}_{i\in\mathbb{N}} \{\gamma_{\text{DL}}^{\text{HD}}(i), \gamma_{\text{UL}}^{\text{HD}}(i)\}$. Note that f' can be different from f because the HD mode downlink SINR $\gamma_{\text{DL}}^{\text{HD}}(i)$ in (6) is different from the conservative SINR $\hat{\gamma}_{\text{DL}}^{\text{FD}}(i)$ in (7), which is used to select user f.

Incorporating Fairness: While UPSMA is designed to maximize the sum spectral efficiency, user fairness can also be incorporated in it. For example, instead of choosing the user that maximizes the instantaneous SINR in Step 1, the user that maximizes the ratio of the instantaneous rate to the average or weighted average rate thus far can be selected, as is done in proportional fair scheduling. The criteria in subsequent steps can also be modified accordingly.

IV. Spectral Efficiency of UPSMA With Index-Only Feedback

We now analyze the uplink, downlink, and sum spectral efficiencies of UPSMA. To gain analytical insights, we focus on index-only feedback ($b = 0$) for the single-cell scenario ($I_{\text{BS}} = I_d = 0$) with perfect SI suppression ($\Delta = \infty$). This gives a lower bound on the sum spectral efficiency for $b \geq 1$ bits. The analysis is intractable for $b \geq 1$ because the inter-user interference is a random RV and it makes the uplink and downlink spectral efficiencies dependent on each other. We shall numerically assess the impact of b and Δ in Section V.

The FD mode uplink and conservative downlink SINRs for user i in (3) and (7), both of which depend on h_i, simplify to

$$\gamma_{\text{UL}}^{\text{FD}}(i) = \frac{P_{\text{U}} h_i}{\sigma_{\text{ul}}^2} \quad \text{and } \hat{\gamma}_{\text{DL}}^{\text{FD}}(i) = \frac{P_{\text{BS}} h_i}{\gamma_{\text{th}} + \sigma_{\text{dl}}^2}. \tag{10}$$

We first evaluate the probability $\mathbb{P}(\mathcal{B}_f)$ that the set $\mathcal{B}_f$ is fed back when user $f \in \mathbb{N}$ is scheduled first. The following two scenarios arise depending on $|\mathcal{B}_f|$:

i) When $|\mathcal{B}_f| < L$: In this case, user $i \notin \mathcal{B}_f$ if and only if $P_{\text{U}} g_{f,i} > \gamma_{\text{th}}$. Hence,

$$\begin{aligned}\mathbb{P}(\mathcal{B}_f) &= \mathbb{P}\left(P_{\text{U}} g_{f,i} \leq \gamma_{\text{th}}, \forall i \in \mathcal{B}_f;\right. \\ &\qquad \left. P_{\text{U}} g_{f,i} > \gamma_{\text{th}}, \forall i \in \mathbb{N} \setminus (\mathcal{B}_f \cup \{f\})\right), \\ &= \left[\prod_{k\in\mathcal{B}_f} F_{g_{f,k}}\left(\frac{\gamma_{\text{th}}}{P_{\text{U}}}\right)\right] \\ &\quad \times \left[\prod_{i\in\mathbb{N}\setminus(\mathcal{B}_f\cup\{f\})} \left(1 - F_{g_{f,i}}\left(\frac{\gamma_{\text{th}}}{P_{\text{U}}}\right)\right)\right]. \end{aligned} \tag{11}$$

ii) When $|\mathcal{B}_f| = L$: In this case, there are at least L users whose inter-user interference to f is less than or equal to γ_{th}. Thus, $\mathcal{B}_f$ contains the L users with the lowest interferences, or, equivalently, inter-user channel gains. Let user k cause the largest interference among the users in $\mathcal{B}_f$. This means that: (i) $g_{f,i} \leq g_{f,k}$, $\forall i \in \mathcal{B}_f \setminus \{k\}$, (ii) $g_{f,k} \leq g_{f,i}$,

$\forall i \in \mathbb{N} \setminus (\mathcal{B}_f \cup \{f\})$, and (iii) $P_{\mathrm{U}} g_{f,k} \leq \gamma_{\mathrm{th}}$. Considering all the possibilities for k, we get

$$\mathbb{P}(\mathcal{B}_f) = \sum_{k \in \mathcal{B}_f} \mathbb{P}\left(g_{f,i} \leq g_{f,k}, \forall i \in \mathcal{B}_f \setminus \{k\}; \right. \\ \left. g_{f,k} \leq g_{f,i}, \forall i \in \mathbb{N} \setminus (\mathcal{B}_f \cup \{f\}); P_{\mathrm{U}} g_{f,k} \leq \gamma_{\mathrm{th}}\right). \tag{12}$$

Conditioning on $g_{f,k}$ and then averaging over it, we get

$$\mathbb{P}(\mathcal{B}_f) = \sum_{k \in \mathcal{B}_f} \int_0^{\frac{\gamma_{\mathrm{th}}}{P_{\mathrm{U}}}} f_{g_{f,k}}(x) \left[\prod_{i \in \mathcal{B}_f \setminus \{k\}} F_{g_{f,i}}(x)\right] \\ \times \left[\prod_{i \in \mathbb{N} \setminus (\mathcal{B}_f \cup \{f\})} \left(1 - F_{g_{f,i}}(x)\right)\right] dx. \tag{13}$$

A. Spectral Efficiency Analysis

We see from (10) that if $P_{\mathrm{U}}/\sigma_{\mathrm{ul}}^2 > P_{\mathrm{BS}}/\left(\gamma_{\mathrm{th}} + \sigma_{\mathrm{dl}}^2\right)$, then for any user, its FD mode uplink SINR is greater than its conservative FD mode downlink SINR. Therefore, f will be an uplink user. We shall refer to this as the *uplink first case*. Else, f is a downlink user, which we shall refer to as the *downlink first case*. The following result gives the uplink spectral efficiency C_{UL} and the downlink spectral efficiency C_{DL} for each case. For tractability, these are derived assuming that the HD mode is selected only if $\mathcal{B}_f = \emptyset$. In effect, the sum of these expressions lower bounds the sum spectral efficiency of UPSMA.

Result 1: In the uplink first case,

$$C_{\mathrm{UL}} = \sum_{i \in \mathbb{N}} \int_0^{\infty} \log_2(1+\gamma) f_{\gamma_{\mathrm{UL}}^{\mathrm{FD}}(i)}(\gamma) \\ \times \left[\prod_{j=1, j \neq i}^{N} F_{\gamma_{\mathrm{UL}}^{\mathrm{FD}}(j)}(\gamma)\right] d\gamma, \tag{14}$$

and

$$C_{\mathrm{DL}} = \sum_{f \in \mathbb{N}} \sum_{\mathcal{B}_f \neq \emptyset} \mathbb{P}(\mathcal{B}_f) \left(\sum_{s \in \mathcal{B}_f} \int_0^{\infty} \log_2(1+\gamma) f_{\hat{\gamma}_{\mathrm{DL}}^{\mathrm{FD}}(s)}(\gamma) \right. \\ \times \left[\prod_{i \in \mathcal{B}_f \setminus \{s\}} F_{\hat{\gamma}_{\mathrm{DL}}^{\mathrm{FD}}(i)}(\gamma)\right] \int_{\gamma}^{\infty} f_{\hat{\gamma}_{\mathrm{DL}}^{\mathrm{FD}}(f)}(x) \\ \left. \times \left[\prod_{i \in \mathbb{N} \setminus (\mathcal{B}_f \cup \{f\})} F_{\hat{\gamma}_{\mathrm{DL}}^{\mathrm{FD}}(i)}(x)\right] dx\, d\gamma \right). \tag{15}$$

In the downlink first case,

$$C_{\mathrm{UL}} = \sum_{f \in \mathbb{N}} \sum_{\mathcal{B}_f \neq \emptyset} \mathbb{P}(\mathcal{B}_f) \left(\sum_{s \in \mathcal{B}_f} \int_0^{\infty} \log_2(1+\gamma) \right. \\ \times f_{\gamma_{\mathrm{UL}}^{\mathrm{FD}}(s)}(\gamma) \left[\prod_{i \in \mathcal{B}_f \setminus \{s\}} F_{\gamma_{\mathrm{UL}}^{\mathrm{FD}}(i)}(\gamma)\right] \int_{\gamma}^{\infty} f_{\gamma_{\mathrm{UL}}^{\mathrm{FD}}(f)}(x) \\ \left. \times \left[\prod_{i \in \mathbb{N} \setminus (\mathcal{B}_f \cup \{f\})} F_{\gamma_{\mathrm{UL}}^{\mathrm{FD}}(i)}(x)\right] dx\, d\gamma \right), \tag{16}$$

and

$$C_{\mathrm{DL}} = \sum_{i \in \mathbb{N}} \int_0^{\infty} \log_2(1+\gamma) f_{\hat{\gamma}_{\mathrm{DL}}^{\mathrm{FD}}(i)}(\gamma) \\ \times \left[\prod_{j=1, j \neq i}^{N} F_{\hat{\gamma}_{\mathrm{DL}}^{\mathrm{FD}}(j)}(\gamma)\right] d\gamma. \tag{17}$$

Proof: The proof is given in Appendix A. ■

The sum spectral efficiency is given by $C_{\mathrm{UL}} + C_{\mathrm{DL}}$. The CDFs $F_{\gamma_{\mathrm{UL}}^{\mathrm{FD}}(i)}(\gamma)$ and $F_{\hat{\gamma}_{\mathrm{DL}}^{\mathrm{FD}}(i)}(\gamma)$ depend on the channel model. While the above expressions apply to the general scenario in which the users are at different distances from the BS and also from each other, they are involved and require the integrals to be computed numerically or using Gauss quadrature techniques [30, Ch. 19.5]. To gain insights about how to choose γ_{th} and how the uplink and downlink spectral efficiencies scale with the number of users N, we study the asymptotic regime in which N is large, and $\mu_1 = \cdots = \mu_N = \mu'$ and $\mu_{m,n} = \mu''$, for $m, n \in \mathbb{N}$ and $m \neq n$ [7].

B. Asymptotic Behavior

We consider the fading-pathloss and fading-shadowing-pathloss models separately below.

1) Fading-Pathloss Model: The following lemma characterizes the scaling law for γ_{th}.

Lemma 1: Let $L \leq \left[(N-1)/\left(2N^{\zeta}\right)\right]^{\kappa}$, for any $0 < \kappa < 1$, and

$$\gamma_{\mathrm{th}} = \frac{P_{\mathrm{U}} \mu''}{N^{\zeta}}, \quad \text{for } \zeta > 0. \tag{18}$$

Then, as $N \to \infty$, $\mathbb{P}(|\mathcal{B}_f| < L) \to 0$ when $0 < \zeta < 1$, and $\mathbb{P}(|\mathcal{B}_f| = 0) \to 1$ when $\zeta > 1$.

Proof: The proof is given in Appendix B. ■

Lemma 1 implies that γ_{th} should not decrease at a rate faster than $P_{\mathrm{U}}\mu''/N$ because $|\mathcal{B}_f|$ becomes 0 with probability 1. This causes the BS to switch to the HD mode, which is sub-optimal. So long as γ_{th} decreases at a rate slower than $P_{\mathrm{U}}\mu''/N$, $|\mathcal{B}_f|$ is L with probability 1. This enables the BS to exploit multi-user diversity to the maximum extent allowed by the feedback constraints while scheduling the second user. We also note that a fixed L, i.e., a fixed feedback overhead, is a special case of $L \leq \left[(N-1)/\left(2N^{\zeta}\right)\right]^{\kappa}$ when $0 < \zeta, \kappa < 1$. The lemma also implies that the constants ζ and κ can take a range of values.

The uplink and downlink spectral efficiencies then scale as follows.

Result 2: Let $\gamma_{\mathrm{th}} = P_{\mathrm{U}}\mu''/N^{\zeta}$, for any $0 < \zeta < 1$, and $L \leq \left[(N-1)/\left(2\,N^{\zeta}\right)\right]^{\kappa}$, for any $0 < \kappa < 1$. Then, in the uplink first case,

$$C_{\mathrm{UL}} = \log_2\left(\frac{P_{\mathrm{U}}\mu'}{\sigma_{\mathrm{ul}}^2}\right) + \log_2(\log(N)) + O\left(\log(\log(\log(N)))\right), \tag{19}$$

and

$$\log_2\left(1+\frac{P_{\text{BS}}\mu'}{\sigma_{\text{dl}}^2}\exp\left(-E\right)\right) \le C_{\text{DL}} \le L\log_2(e)\exp\left(\frac{\sigma_{\text{dl}}^2}{P_{\text{BS}}\mu'}\right) \times\left[\frac{\sigma_{\text{dl}}^2}{P_{\text{BS}}\mu'}-\log\left(\frac{\sigma_{\text{dl}}^2}{P_{\text{BS}}\mu'}\right)-E\right]. \quad (20)$$

In the downlink first case,

$$C_{\text{DL}}=\log_2\left(\frac{P_{\text{BS}}\mu'}{\sigma_{\text{dl}}^2}\right)+\log_2(\log(N))+O\left(\log(\log(\log(N)))\right), \quad (21)$$

and

$$\log_2\left(1+\frac{P_{\text{U}}\mu'}{\sigma_{\text{ul}}^2}\exp\left(-E\right)\right) \le C_{\text{UL}} \le L\log_2(e)\exp\left(\frac{\sigma_{\text{ul}}^2}{P_{\text{U}}\mu'}\right) \times\left[\frac{\sigma_{\text{ul}}^2}{P_{\text{U}}\mu'}-\log\left(\frac{\sigma_{\text{ul}}^2}{P_{\text{U}}\mu'}\right)-E\right]. \quad (22)$$

Proof: The proof is given in Appendix C. ∎

In the uplink first case, C_{UL} and the spectral efficiency of an HD system [31] both scale as $\log(\log(N))$. This is intuitive because the uplink user is selected from among all the N users. On the other hand, C_{DL} is a constant due to feedback constraints. Similarly, in the downlink first case, C_{DL} scales as $\log(\log(N))$ while C_{UL} is a constant.

2) Fading-Shadowing-Pathloss Model: For the fading-shadowing-pathloss model, the channel gains are Suzuki RVs. A Suzuki RV can be well approximated by a lognormal RV since the shadowing dominates the small-scale fading [32]. Let $\tilde{\mu}'$ be the dB-mean of the lognormal RV that approximates the channel gain between the BS and a user, and $\tilde{\mu}''$ be the corresponding dB-mean for an inter-user channel gain. And, let $\tilde{\sigma}_{\text{dB}}$ be their dB-standard deviation.[1] Then, the scaling law for γ_{th} is as follows.

Lemma 2: Let $L \le (N-1)^{\kappa'}\left[1-Q\left(\zeta'\sqrt{2\log(N)}\right)\right]^{\kappa'}$, for any $0<\kappa'<1$, and γ_{th} be set as a function of N as

$$\gamma_{\text{th}} = P_{\text{U}}\exp\left(\frac{\tilde{\mu}''}{\xi}-\frac{\zeta'\tilde{\sigma}_{\text{dB}}}{\xi}\sqrt{2\log(N)}\right), \quad \text{for } \zeta'>0, \quad (23)$$

where $\xi = 10/\log(10)$. Then, as $N\to\infty$, $\mathbb{P}\left(|\mathcal{B}_f|<L\right)\to 0$ for any $0<\zeta'<1$, and $\mathbb{P}\left(|\mathcal{B}_f|=0\right)\to 1$ for any $\zeta'>1$.

Proof: The proof is given in Appendix D. ∎

ζ' and κ' are arbitrary constants. If γ_{th} decreases at a rate faster than $\exp\left(-\zeta'\tilde{\sigma}_{\text{dB}}\sqrt{2\log(N)}/\xi\right)$, then $|\mathcal{B}_f|\to 0$ with probability 1. Otherwise, $|\mathcal{B}_f|\to L$ with probability 1. This behavior is different from Lemma 1. The uplink and downlink spectral efficiencies then scale as follows.

[1]We use the moment generation function (MGF) matching method of [32] to determine $\tilde{\mu}'$, $\tilde{\mu}''$, and $\tilde{\sigma}_{\text{dB}}$. It uses two parameters s_1 and s_2, which are set as $s_1=0.35$ and $s_2=0.55$.

Result 3: Let $\gamma_{\text{th}} = P_{\text{U}}\exp\left(\left[\tilde{\mu}''-\zeta'\tilde{\sigma}_{\text{dB}}\sqrt{2\log(N)}\right]/\xi\right)$, for any $0<\zeta'<1$, and $L \le (N-1)^{\kappa'}\left[1-Q\left(\zeta'\sqrt{2\log(N)}\right)\right]^{\kappa'}$, for any $0<\kappa'<1$. In the uplink first case,

$$C_{\text{UL}} = \log_2\left(\frac{P_{\text{U}}}{\sigma_{\text{ul}}^2}\exp\left(\frac{\tilde{\mu}'}{\xi}\right)\right)+\frac{\tilde{\sigma}_{\text{dB}}\log_2(e)}{\xi}\sqrt{2\log(N)} +O(\log(\log(N))), \quad (24)$$

and

$$\log_2\left(1+\frac{P_{\text{BS}}}{\sigma_{\text{dl}}^2}\exp\left(\frac{\tilde{\mu}'}{\xi}\right)\right) \le C_{\text{DL}} \le L\log_2\left(1+\frac{P_{\text{BS}}}{\sigma_{\text{dl}}^2}\exp\left(\frac{\tilde{\mu}'}{\xi}+\frac{\tilde{\sigma}_{\text{dB}}^2}{2\xi^2}\right)\right). \quad (25)$$

In the downlink first case,

$$C_{\text{DL}} = \log_2\left(\frac{P_{\text{BS}}}{\sigma_{\text{dl}}^2}\exp\left(\frac{\tilde{\mu}'}{\xi}\right)\right)+\frac{\tilde{\sigma}_{\text{dB}}\log_2(e)}{\xi}\sqrt{2\log(N)} +O(\log(\log(N))), \quad (26)$$

and

$$\log_2\left(1+\frac{P_{\text{U}}}{\sigma_{\text{ul}}^2}\exp\left(\frac{\tilde{\mu}'}{\xi}\right)\right) \le C_{\text{UL}} \le L\log_2\left(1+\frac{P_{\text{U}}}{\sigma_{\text{ul}}^2}\exp\left(\frac{\tilde{\mu}'}{\xi}+\frac{\tilde{\sigma}_{\text{dB}}^2}{2\xi^2}\right)\right). \quad (27)$$

Proof: The proof is given in Appendix E. ∎

The scaling behavior is different from that for the fading-pathloss model. As before, either C_{UL} or C_{DL} scales as the spectral efficiency of an HD system[2] and the other saturates to a constant due to feedback constraints.

V. Simulation Results and Benchmarking

We now present simulation results for single-cell and multi-cell scenarios with the two channel models. The Monte Carlo simulations are averaged over 10^6 channel realizations. The simulation parameters are set as follows: cell radius R is 100 m, bandwidth is 1 MHz, $\eta=3.7$, $K=-40$ dB, $d_0=1$ m, noise power spectral density is -174 dBm/Hz, noise figure at the BS and the users is 10 dB, and $\sigma_{\text{dB}}=8$. We choose P_{BS} so that the fading-averaged downlink cell-edge SNR is 0 dB and we set $P_{\text{U}}=P_{\text{BS}}$ unless specified otherwise. In order to asses the efficacy of the algorithms for statistically non-identical channels, we set user i to be at a distance of iR/N from the BS and at an azimuth angle $2\pi i/N$. To determine the quantization thresholds for $b\ge 1$, we set $G=5$ dB. This value is numerically found to maximize the sum spectral efficiency.

In the multi-cell scenario, results for which are shown in Section V-B, we benchmark the sum spectral efficiency of UPSMA with the following scheduling and mode selection algorithms:

1) *HD System:* In it, the BS either transmits to a user or receives from it, but it does not do both simultaneously.

[2]It can be shown using an analysis similar to ours that the spectral efficiency of an HD system scales as $\Theta(\sqrt{\log(N)})$. To the best of our knowledge, this result is also not available in the literature.

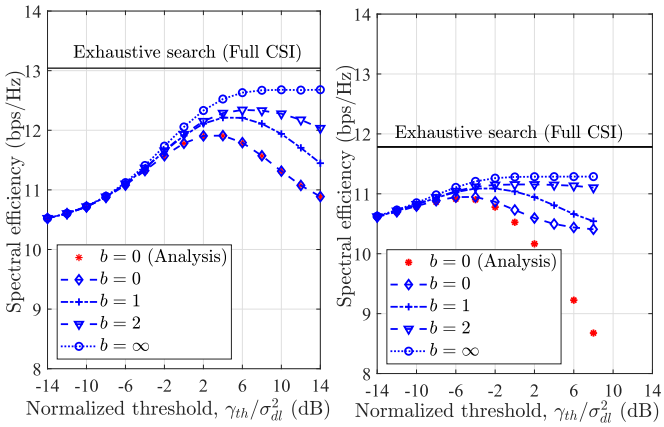

(a) Uplink first case (b) Downlink first case

Fig. 2. Fading-pathloss model and single-cell scenario: Sum spectral efficiency as a function of the normalized threshold $\gamma_{\text{th}}/\sigma_{\text{dl}}^2$ ($N = 8$, $L = 4$, and $\Delta = \infty$).

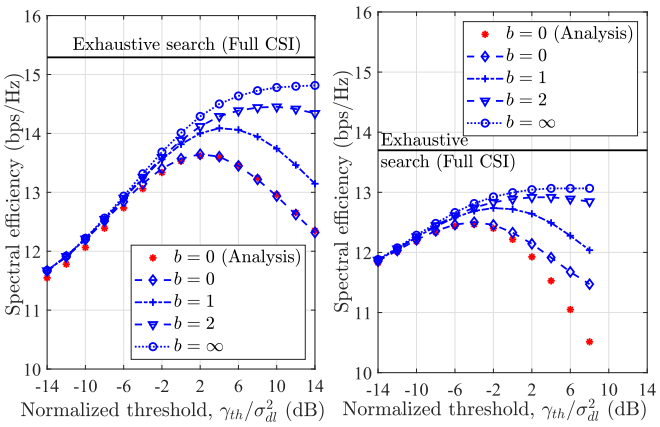

(a) Uplink first case (b) Downlink first case

Fig. 3. Fading-shadowing-pathloss model and single-cell scenario: Sum spectral efficiency as a function of the normalized threshold, $\gamma_{\text{th}}/\sigma_{\text{dl}}^2$ ($N = 8$, $L = 4$, and $\Delta = \infty$).

The user with the highest SINR – be it on the uplink or the downlink – is scheduled. This maximizes the HD spectral efficiency since the user with the maximum of the uplink and downlink spectral efficiencies is selected.

2) *Exhaustive Search:* All the inter-user channel gains are assumed to be known to the BS with infinite resolution. The uplink and downlink user-pair with the largest sum spectral efficiency among all the user-pairs is determined. Its sum spectral efficiency is compared with that of the HD mode, and the mode with the highest sum spectral efficiency is used.
3) *AKA-1, 2, and 3 [7]:* These algorithms are described in Section I-A. To adapt to our system model and to ensure a fair comparison, two users with the largest and second largest channel gains are scheduled on the uplink and the downlink in AKA-1. And, in AKA-2 and AKA-3, the BS knows only the L lowest interferences to the first scheduled user and the users that cause them. It knows these with infinite resolution.

We note that a comparison with the user-pair scheduling algorithms in [11], [13], [14] is not possible because these algorithms assume that BS knows the inter-user interference of all user-pairs. On the other hand, limited feedback, user pairing, and scheduling are intimately connected in UPSMA.

A. Single-Cell Scenario

Fig. 2 plots the sum spectral efficiency of UPSMA as a function of the normalized threshold $\gamma_{\text{th}}/\sigma_{\text{dl}}^2$ in dB-scale for different numbers of feedback bits b for the fading-pathloss model. Fig. 2(a) plots this for the uplink first case, and Fig. 2(b) for the downlink first case. When $P_{\text{BS}} = P_{\text{U}}$, it follows from (10) that the FD mode uplink SINR exceeds the conservative FD mode downlink SINR. Thus, the uplink first case occurs in UPSMA. For the downlink first case in Fig. 2(b), we reduce P_{U} by 9 dB, while keeping P_{BS} the same. Fig. 3 shows the corresponding results for the fading-shadowing-pathloss model. For the downlink first case in Fig. 2(b) and Fig. 3(b), results are shown only for $\gamma_{\text{th}}/\sigma_{\text{dl}}^2 \leq 8$ dB since the uplink first case applies for larger values.

For $b = 0$, 1, and 2 bits, as γ_{th} increases, the sum spectral efficiency increases, reaches a peak, and then decreases. This is because when γ_{th} is small, $|\mathcal{B}_f|$ is often less than L as there are few users whose inter-user interference is below γ_{th}. As a result, the BS has considerably less choice in scheduling the second user. On the other hand, when γ_{th} is large, $|\mathcal{B}_f| = L$ with high probability, but the larger inter-user interference reduces the downlink SINR. The behavior is different for $b = \infty$ bits. In this case, γ_{th} only affects $|\mathcal{B}_f|$. As γ_{th} increases, the sum spectral efficiency increases because a large $|\mathcal{B}_f|$ becomes more probable. Once $|\mathcal{B}_f|$ is L with high probability, the sum spectral efficiency saturates. As b increases, the sum spectral efficiency increases due to the increased resolution of the feedback. Thus, the feedback overhead and γ_{th} have a significant impact on the system's performance.

At the optimal value of γ_{th}, the sum spectral efficiency is within 8.6%, 6.3%, and 5.3% of that of exhaustive search for $b = 0$, 1, and 2 bits, respectively, for both uplink and downlink first cases for the fading-pathloss model. The corresponding numbers for the fading-shadowing-pathloss model are 10.7%, 7.8%, and 5.6%. Also plotted in each subfigure is the curve from analysis for index-only feedback. The analytical curve is close to the simulation curve when $\gamma_{\text{th}}/\sigma_{\text{dl}}^2$ is below the optimal value, and is below the simulation curve at larger values of $\gamma_{\text{th}}/\sigma_{\text{dl}}^2$. This is clearly visible for the downlink first case. This is because the BS reverts to the HD mode more often in Step 3 as γ_{th} increases and the conservative FD mode downlink SINR decreases. As discussed in Section IV-A, this step is not accounted for in the analysis. For the uplink first case, it can be shown that the FD mode spectral efficiency is always greater than or equal to the HD mode spectral efficiency. Hence, the BS does not revert to the HD mode in the third step and there is no gap between the analysis and simulation curves.

Asymptotic Behavior: We show results for the uplink first case henceforth. Fig. 4 studies the asymptotic scaling behavior of the optimal threshold, which maximizes the sum spectral efficiency, for index-only feedback for different values of L. The optimal threshold is found using a numerical search. Fig. 4(a) plots optimal $\gamma_{\text{th}}/\sigma_{\text{dl}}^2$ in dB scale as a function of $\log(N)$ for the fading-pathloss model. Fig. 4(b) plots optimal

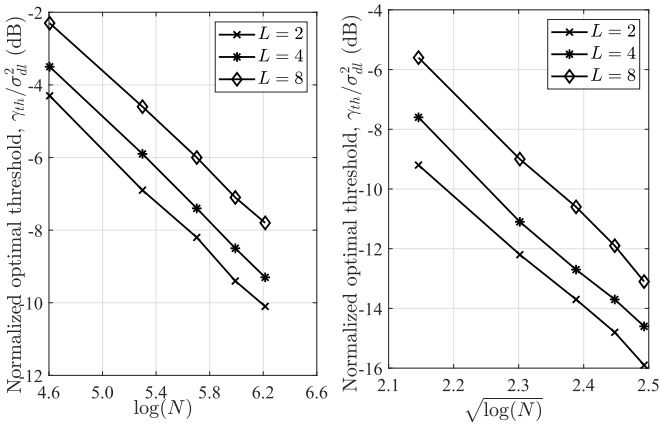

(a) Fading-pathloss model. (b) Fading-shadowing-pathloss model

Fig. 4. Single-cell scenario: Asymptotic scaling behavior of optimal value of $\gamma_{\text{th}}/\sigma_{\text{dl}}^2$ (Uplink first case, $\mu' = -94.0$ dB, $\mu'' = -105.1$ dB, and $\Delta = \infty$).

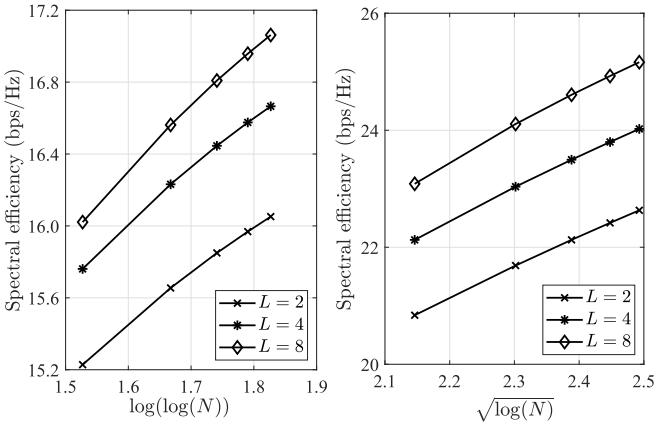

(a) Fading-pathloss model (b) Fading-shadowing-pathloss model

Fig. 5. Single-cell scenario: Asymptotic scaling behavior of sum spectral efficiency (Uplink first case, $\mu' = -94$ dB, $\mu'' = -105.1$ dB, and $\Delta = \infty$).

$\gamma_{\text{th}}/\sigma_{\text{dl}}^2$ in dB scale as a function of $\sqrt{\log(N)}$ for the fading-shadowing-pathloss model. The near-linear shape of the curves verifies the scaling laws of Lemmas 1 and 2. The optimal value of γ_{th} decreases as L increases. This occurs in order to increase the odds that there are sufficient number of users whose inter-user interferences are below γ_{th} and, thus, can be included in $\mathcal{B}_f$. For any N, the optimal value of γ_{th} is lower in the fading-shadowing-pathloss model because the fluctuations due to shadowing increase the probability of finding users with lower inter-user interferences.

Fig. 5(a) plots the asymptotic sum spectral efficiency as a function of $\log(\log(N))$ for the fading-pathloss model for different L. This is done using the optimal value for γ_{th}, which is taken from Fig. 4(a). The corresponding results for the fading-shadowing-pathloss model are shown in Fig. 5(b), which plots the sum spectral efficiency as a function of $\sqrt{\log(N)}$. In this case, the optimal values for γ_{th} are taken from Fig. 4(b). The near-linear behavior of the curves verifies the scaling laws in Results 2 and 3. The sum spectral efficiency is larger and increases at a faster rate as N increases for the fading-shadowing-pathloss model. Thus, the increased fluctuations due to shadowing improve the spectral efficiency.

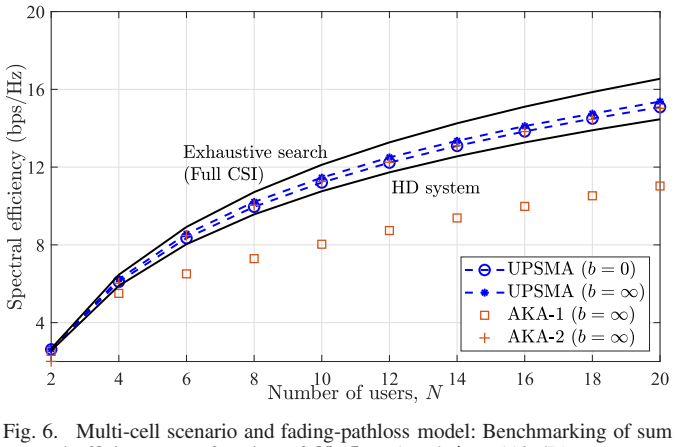

Fig. 6. Multi-cell scenario and fading-pathloss model: Benchmarking of sum spectral efficiency as a function of N ($L = 4$ and $\Delta = 110$ dB).

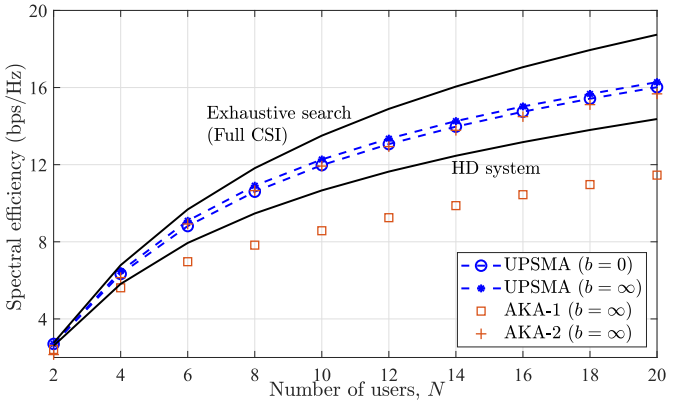

Fig. 7. Multi-cell scenario and fading-shadowing-pathloss model: Benchmarking of sum spectral efficiency as a function of N ($L = 4$ and $\Delta = 110$ dB).

It increases as N increases because of the multi-user diversity. It also increases as L increases because more CSI is fed back.

B. Multi-Cell Scenario and Performance Benchmarking

We now present results for a multi-cell scenario that consists of 19 cells that are laid out in a two-tier hexagonal cellular layout. Now, co-channel interference occurs at the BS on the uplink and at the users on the downlink. We also model imperfect SI suppression. As a result, the uplink first and downlink first cases can both occur for any value of P_{U} and P_{BS}. For each N, the values of γ_{th} are obtained by numerically optimizing the sum spectral efficiency for $b = 0$ bits and the same values are used for $b = \infty$ bits.

Fig. 6 plots the sum spectral efficiency of UPSMA with $b = 0$ bits and $b = \infty$ bits, exhaustive search, AKA-1, AKA-2, and HD system for the fading-pathloss model.[3] The corresponding results for the fading-shadowing-pathloss model are shown in Fig. 7. The trends in the two figures are qualitatively similar. The sum spectral efficiency of UPSMA with index-only feedback ($b = 0$) is more than that of the HD system and AKA-1, which does not account for the inter-user interference. It is comparable to that of AKA-2, even though the lowest L inter-user interferences are assumed to be

[3]To avoid clutter, results for AKA-3 are not shown as they are close to those of AKA-2. For UPSMA, results for $b = 1$ and $b = 2$ are not shown as their curves are close to the other curves.

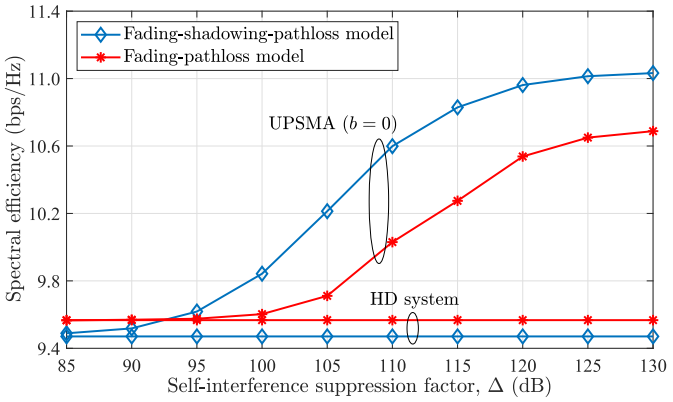

Fig. 8. Multi-cell scenario: Zoomed-in view of sum spectral efficiency as a function of SI suppression factor Δ ($L = 4$, $b = 0$, and $N = 8$).

available to the BS with infinite resolution. This is because of two reasons. First, AKA-2 does not account for inter-cell interference when it selects the downlink user, though it accounts for it while determining the uplink and downlink data rates. Second, AKA-2 always chooses an uplink user first. As b increases, the sum spectral efficiency of UPSMA increases for both channel models. At $b = \infty$ bits, it is within 6.6% and 12.9% of that of exhaustive search for the fading-pathloss and fading-shadowing-pathloss models, respectively.

Fig. 8 plots the sum spectral efficiency of UPSMA as a function of the SI suppression factor Δ. Also shown is the spectral efficiency of the HD system, which is a horizontal line as it does not depend on Δ. The spectral efficiencies of UPSMA and the HD system are the same for $\Delta \leq 95$ dB for the fading-pathloss model. This happens for $\Delta \leq 85$ dB for the fading-shadowing-pathloss model. When Δ is small, the large SI makes UPSMA to choose the HD mode with a high probability. As Δ increases and the SI power becomes comparable to the co-channel interference plus noise power, the spectral efficiency of UPSMA increases and eventually saturates. Thus, the FD capability at the BS can appreciably increase the spectral efficiency, but cannot double it due to feedback constraints and inter-user interference. The presence of shadowing increases the spectral efficiency of UPSMA, but the reverse is true for the HD system.

VI. Conclusion

We proposed a novel user-pair scheduling and mode selection algorithm and a scheme to feed back quantized information about a limited number of users whose inter-user interferences were below a threshold γ_{th}. This enabled the BS to lower bound the SINR for the downlink user even when it was yet to determine the uplink user. We saw that γ_{th} and the maximum feedback set size L had a significant influence on the FD system performance. A larger γ_{th} increased the number of users who could be included in the feedback set, but also led to a larger inter-user interference. On the other hand, a smaller γ_{th} increased the downlink SINR, but reduced the number of users that the scheduler could choose from. The asymptotic scaling laws revealed how the optimal threshold and the uplink and downlink spectral efficiencies scaled as a function of the number of users. They were different for the fading-pathloss and fading-shadowing-pathloss models. Numerical results, which accounted for co-channel interference and imperfect SI suppression, showed that the sum spectral efficiency of UPSMA was close to that of exhaustive search and conventional algorithms that assumed the availability of more CSI at the BS.

Appendix

A. Brief Proof of Result 1

1) Uplink First Case: We first evaluate C_{UL} and then C_{DL}.

a) Evaluation of C_{UL}: Let γ_{UL} denote the uplink SINR. In the uplink first case, the first scheduled user f has the largest FD mode uplink SINR among all the N users. Hence, the CDF $F_{\gamma_{\text{UL}}}(\gamma)$ of γ_{UL} is given by

$$F_{\gamma_{\text{UL}}}(\gamma) = \mathbb{P}\left(\max_{i\in\mathbb{N}}\left\{\gamma_{\text{UL}}^{\text{FD}}(i)\right\} \leq \gamma\right) = \prod_{i\in\mathbb{N}} F_{\gamma_{\text{UL}}^{\text{FD}}(i)}(\gamma). \tag{28}$$

Differentiating $F_{\gamma_{\text{UL}}}(\gamma)$ with respect to γ and substituting it in the formula $C_{\text{UL}} = \int_0^\infty \log_2(1+\gamma) f_{\gamma_{\text{UL}}}(\gamma)\, d\gamma$ yields (14).

b) Evaluation of C_{DL}: Let γ_{DL} represent SINR of the downlink and $\mathbb{P}(\gamma_{\text{DL}} \leq \gamma, f, \mathcal{B}_f, s)$ denote the joint probability of the events $\gamma_{\text{DL}} \leq \gamma$, first scheduled user is f, second scheduled user is s, and feedback set is $\mathcal{B}_f$. If $\mathcal{B}_f = \emptyset$, then no user is scheduled on the downlink, which is mathematically equivalent to $\gamma_{\text{DL}} = 0$. Let $\mathbb{P}(f, \mathcal{B}_f = \emptyset)$ denote the joint probability of the events that the first scheduled user is f and $\mathcal{B}_f = \emptyset$. Then, from the law of total probability, the CDF $F_{\gamma_{\text{DL}}}(\gamma)$ of γ_{DL} is given by

$$F_{\gamma_{\text{DL}}}(\gamma) = \sum_{f\in\mathbb{N}} \sum_{\mathcal{B}_f\neq\emptyset} \sum_{s\in\mathcal{B}_f} \mathbb{P}(\gamma_{\text{DL}} \leq \gamma, f, \mathcal{B}_f, s) + \sum_{f\in\mathbb{N}} \mathbb{P}(f, \mathcal{B}_f = \emptyset). \tag{29}$$

From Bayes' rule, we have

$$\mathbb{P}(\gamma_{\text{DL}} \leq \gamma, f, \mathcal{B}_f, s) = \mathbb{P}(\gamma_{\text{DL}} \leq \gamma, f, s|\mathcal{B}_f)\,\mathbb{P}(\mathcal{B}_f). \tag{30}$$

The downlink user s, which is scheduled second, has the largest FD mode downlink SINR among the users in $\mathcal{B}_f$. Recall that in index-only feedback, the FD mode downlink SINR of a user i is taken to be $\hat{\gamma}_{\text{DL}}^{\text{FD}}(i)$. Therefore,

$$\begin{aligned}&\mathbb{P}(\gamma_{\text{DL}} \leq \gamma, f, s|\mathcal{B}_f)\\ &\quad= \mathbb{P}\left(\hat{\gamma}_{\text{DL}}^{\text{FD}}(s) < \gamma; \hat{\gamma}_{\text{DL}}^{\text{FD}}(s) \geq \hat{\gamma}_{\text{DL}}^{\text{FD}}(i), \forall i \in \mathcal{B}_f \setminus \{s\};\right.\\ &\qquad\left.\gamma_{\text{UL}}^{\text{FD}}(f) \geq \gamma_{\text{UL}}^{\text{FD}}(i), \forall i \in \mathbb{N}\setminus\{f\}\right).\end{aligned} \tag{31}$$

From (10), we see that $\gamma_{\text{UL}}^{\text{FD}}(f) \geq \gamma_{\text{UL}}^{\text{FD}}(i)$ is equivalent to $\hat{\gamma}_{\text{DL}}^{\text{FD}}(f) \geq \hat{\gamma}_{\text{DL}}^{\text{FD}}(i)$. Setting $i = s$, we get $\hat{\gamma}_{\text{DL}}^{\text{FD}}(f) \geq \hat{\gamma}_{\text{DL}}^{\text{FD}}(s)$. For $i \in \mathcal{B}_f$, the condition $\hat{\gamma}_{\text{DL}}^{\text{FD}}(i) \leq \hat{\gamma}_{\text{DL}}^{\text{FD}}(s)$ implies that $\hat{\gamma}_{\text{DL}}^{\text{FD}}(i) \leq \hat{\gamma}_{\text{DL}}^{\text{FD}}(f)$. Conditioning on $\hat{\gamma}_{\text{DL}}^{\text{FD}}(f) = x$ and $\hat{\gamma}_{\text{DL}}^{\text{FD}}(s) = y$ and taking the above points into account, we get

$$\begin{aligned}&\mathbb{P}(\gamma_{\text{DL}} \leq \gamma, f, s|\mathcal{B}_f)\\ &= \mathbb{E}\left[\mathbb{P}\left(\hat{\gamma}_{\text{DL}}^{\text{FD}}(i) \leq y, \forall i \in \mathcal{B}_f\setminus\{s\};\right.\right.\\ &\quad\left.\hat{\gamma}_{\text{DL}}^{\text{FD}}(i) \leq x, \forall i \in \mathbb{N}\setminus(\mathcal{B}_f\cup\{f\})\,|\hat{\gamma}_{\text{DL}}^{\text{FD}}(f) = x, \hat{\gamma}_{\text{DL}}^{\text{FD}}(s) = y\right)\\ &\quad\left.\times 1_{\{y<\gamma\}} 1_{\{x>y\}}\right].\end{aligned} \tag{32}$$

Since $\hat{\gamma}_{\mathrm{DL}}^{\mathrm{FD}}(1), \hat{\gamma}_{\mathrm{DL}}^{\mathrm{FD}}(2), \ldots, \hat{\gamma}_{\mathrm{DL}}^{\mathrm{FD}}(N)$ are mutually independent, we get

$$\begin{aligned}\mathbb{P}&\left(\gamma_{\mathrm{DL}} \leq \gamma, f, s|\mathcal{B}_f\right) \\ &= \int_0^{\gamma} f_{\hat{\gamma}_{\mathrm{DL}}^{\mathrm{FD}}(s)}(y) \left[\prod_{i\in\mathcal{B}_f\setminus\{s\}} F_{\hat{\gamma}_{\mathrm{DL}}^{\mathrm{FD}}(i)}(y)\right] \\ &\quad \times \int_y^{\infty} f_{\hat{\gamma}_{\mathrm{DL}}^{\mathrm{FD}}(f)}(x) \left[\prod_{i\in\mathbb{N}\setminus(\mathcal{B}_f\cup\{f\})} F_{\hat{\gamma}_{\mathrm{DL}}^{\mathrm{FD}}(i)}(x)\right] dx\, dy. \end{aligned} \tag{33}$$

Combining (29), (30), and (33), we get

$$\begin{aligned} F_{\gamma_{\mathrm{DL}}}(\gamma) &= \sum_{f\in\mathbb{N}} \sum_{\mathcal{B}_f\neq\emptyset} \sum_{s\in\mathcal{B}_f} \mathbb{P}(\mathcal{B}_f) \left(\int_0^{\gamma} f_{\hat{\gamma}_{\mathrm{DL}}^{\mathrm{FD}}(s)}(y) \right. \\ &\quad \times \left[\prod_{i\in\mathcal{B}_f\setminus\{s\}} F_{\hat{\gamma}_{\mathrm{DL}}^{\mathrm{FD}}(i)}(y)\right] \int_y^{\infty} f_{\hat{\gamma}_{\mathrm{DL}}^{\mathrm{FD}}(f)}(x) \\ &\quad \left. \times \left[\prod_{i\in\mathbb{N}\setminus(\mathcal{B}_f\cup\{s\})} F_{\hat{\gamma}_{\mathrm{DL}}^{\mathrm{FD}}(i)}(x)\right] dx\, dy\right) \\ &\quad + \sum_{f\in\mathbb{N}} \mathbb{P}(f, \mathcal{B}_f = \emptyset). \end{aligned} \tag{34}$$

Differentiating $F_{\gamma_{\mathrm{DL}}}(\gamma)$ with respect to γ to get $f_{\gamma_{\mathrm{DL}}}(\gamma)$ and substituting it in the expression $C_{\mathrm{DL}} = \int_0^{\infty} \log_2(1+\gamma) f_{\gamma_{\mathrm{DL}}}(\gamma)\, d\gamma$ yields (15).

2) Downlink First Case: We first evaluate C_{DL} and then C_{UL}.

a) Evaluation of C_{DL}: In the downlink first case, $\gamma_{\mathrm{DL}} \leq \gamma$ only if $\hat{\gamma}_{\mathrm{DL}}^{\mathrm{FD}}(i) \leq \gamma$, $\forall i \in \mathbb{N}$. Hence,

$$F_{\gamma_{\mathrm{DL}}}(\gamma) = \prod_{i\in\mathbb{N}} F_{\hat{\gamma}_{\mathrm{DL}}^{\mathrm{FD}}(i)}(\gamma). \tag{35}$$

Differentiating $F_{\gamma_{\mathrm{DL}}}(\gamma)$ with respect to γ and substituting it in $C_{\mathrm{DL}} = \int_0^{\infty} \log_2(1+\gamma) f_{\gamma_{\mathrm{DL}}}(\gamma)\, d\gamma$ yields (17).

b) Evaluation of C_{UL}: Similar to (29), the CDF $F_{\gamma_{\mathrm{UL}}}(\gamma)$ is given by

$$\begin{aligned} F_{\gamma_{\mathrm{UL}}}(\gamma) &= \sum_{f\in\mathbb{N}} \sum_{\mathcal{B}_f\neq\emptyset} \sum_{s\in\mathcal{B}_f} \mathbb{P}(\gamma_{\mathrm{UL}} \leq \gamma, f, \mathcal{B}_f, s) \\ &\quad + \sum_{f\in\mathbb{N}} \mathbb{P}(f, \mathcal{B}_f = \emptyset), \end{aligned} \tag{36}$$

Along lines similar to (34), the CDF $F_{\gamma_{\mathrm{UL}}}(\gamma)$ is given by

$$\begin{aligned} F_{\gamma_{\mathrm{UL}}}(\gamma) &= \sum_{f\in\mathbb{N}} \sum_{\mathcal{B}_f\neq\emptyset} \sum_{s\in\mathcal{B}_f} \mathbb{P}(\mathcal{B}_f) \left(\int_0^{\gamma} f_{\gamma_{\mathrm{UL}}^{\mathrm{FD}}(s)}(y) \right. \\ &\quad \times \left[\prod_{i\in\mathcal{B}_f\setminus\{s\}} F_{\gamma_{\mathrm{UL}}^{\mathrm{FD}}(i)}(y)\right] \int_y^{\infty} f_{\gamma_{\mathrm{UL}}^{\mathrm{FD}}(f)}(x) \\ &\quad \left. \times \left[\prod_{i\in\mathbb{N}\setminus(\mathcal{B}_f\cup\{f\})} F_{\gamma_{\mathrm{UL}}^{\mathrm{FD}}(i)}(x)\right] dx\, dy\right) \\ &\quad + \sum_{f\in\mathbb{N}} \mathbb{P}(f, \mathcal{B}_f = \emptyset). \end{aligned} \tag{37}$$

Differentiating $F_{\gamma_{\mathrm{UL}}}(\gamma)$ with respect to γ and substituting it in $C_{\mathrm{UL}} = \int_0^{\infty} \log_2(1+\gamma_{\mathrm{UL}}) f_{\gamma_{\mathrm{UL}}}(\gamma)\, d\gamma$ yields (16).

B. Proof of Lemma 1

From the law of total probability, we have

$$\mathbb{P}(|\mathcal{B}_f| < L) = \sum_{\mathcal{B}_f:\ |\mathcal{B}_f|<L} \mathbb{P}(\mathcal{B}_f). \tag{38}$$

Substituting the expression for $\mathbb{P}(\mathcal{B}_f)$ from (11) and $F_{g_{m,n}}(x) = 1 - \exp(-x/\mu'')$, for $x \geq 0$, we get

$$\begin{aligned} \mathbb{P}(|\mathcal{B}_f| < L) &= \sum_{\ell=0}^{L-1} \binom{N-1}{\ell} \left(1 - \exp\left(-\frac{\gamma_{\mathrm{th}}}{P_{\mathrm{U}}\mu''}\right)\right)^{\ell} \\ &\quad \times \left(\exp\left(-\frac{\gamma_{\mathrm{th}}}{P_{\mathrm{U}}\mu''}\right)\right)^{N-\ell-1}. \end{aligned} \tag{39}$$

Consider a binomial RV X_N with parameter $p_N = 1 - \exp(-\gamma_{\mathrm{th}}/P_{\mathrm{U}}\mu'')$. It is easy to see that $\mathbb{P}(|\mathcal{B}_f| < L) = \mathbb{P}(X_N < L)$. When $p_N \to 0$ and $Np_N \to \infty$, we know that [33, Ch. 3.3] $(X_N - Np_N)/\sqrt{Np_N(1-p_N)} \xrightarrow{d} \mathcal{N}(0,1)$. Therefore,

$$\begin{aligned} &\mathbb{P}(|\mathcal{B}_f| < L) \\ &= \mathbb{P}(X_N < L) \\ &\to 1 - Q\left(\frac{L - (N-1)\left[1 - \exp\left(-\frac{\gamma_{\mathrm{th}}}{P_{\mathrm{U}}\mu''}\right)\right]}{\sqrt{(N-1)\left[1 - \exp\left(-\frac{\gamma_{\mathrm{th}}}{P_{\mathrm{U}}\mu''}\right)\right]\exp\left(-\frac{\gamma_{\mathrm{th}}}{P_{\mathrm{U}}\mu''}\right)}}\right). \end{aligned} \tag{40}$$

Let ζ and κ be two constants such that $0 < \zeta, \kappa < 1$. And, let $\gamma_{\mathrm{th}} = P_{\mathrm{U}}\mu''/N^{\zeta}$. Then, the term inside the Q-function can be shown to converge to $-\infty$ when $L \leq \left[(N-1)/\left(2\,N^{\zeta}\right)\right]^{\kappa}$. Therefore, $\mathbb{P}(|\mathcal{B}_f| < L) \to 1 - Q(-\infty) = 0$.

Now, consider the case where $\zeta > 1$. Substituting $\gamma_{\mathrm{th}} = P_{\mathrm{U}}\mu''/N^{\zeta}$ in (11), we get $\mathbb{P}(|\mathcal{B}_f| = 0) = \exp\left(-(N-1)/N^{\zeta}\right) \to 1$.

C. Proof of Result 2

1) Uplink First Case: We first study the scaling behavior of C_{UL} and then C_{DL}.

a) Scaling Behavior of C_{UL}: We have $\gamma_{\mathrm{UL}} = \max_{i\in\mathbb{N}}\{\gamma_{\mathrm{UL}}^{\mathrm{FD}}(i)\}$. From (1) and (10), we get

$$\gamma_{\mathrm{UL}} = \frac{P_{\mathrm{U}}\mu'}{\sigma_{\mathrm{ul}}^2} \max_{i\in\mathbb{N}}\{\alpha_i\}. \tag{41}$$

The maximum $\max_{i\in\mathbb{N}}\{\alpha_i\}$ of N independent and identically distributed (i.i.d.) exponential RVs with unit means satisfies the following probability bound [31, (A10)]:

$$\begin{aligned} \mathbb{P}\Big(&\log(N) - \log(\log(N)) + O(\log(\log(\log(N)))) \\ &\leq \max_{i\in\mathbb{N}}\{\alpha_i\} \\ &\leq \log(N) + \log(\log(N)) + O(\log(\log(\log(N))))\Big) \\ &> 1 - O\left(\frac{1}{\log(N)}\right). \end{aligned} \tag{42}$$

As $N \to \infty$, $1/\log(N) \to 0$. Therefore, $\max_{i\in\mathbb{N}}\{\alpha_i\} = \log(N) + O(\log(\log(N)))$ with probability 1. Hence, $C_{\text{UL}} = \mathbb{E}[\log_2(1+\gamma_{\text{UL}})] = \log_2\left(P_{\text{U}}\mu'/\sigma_{\text{ul}}^2\right) + \log_2(\log(N)) + O(\log(\log(\log(N))))$.

b) Scaling Behavior of C_{DL}: From the law of total probability, C_{DL} is given by

$$C_{\text{DL}} = \sum_{f\in\mathbb{N}}\sum_{\mathcal{B}_f}\mathbb{P}(f,\mathcal{B}_f)\,T_{\text{DL}}(f,\mathcal{B}_f), \tag{43}$$

where $T_{\text{DL}}(f,\mathcal{B}_f)$ is the downlink spectral efficiency conditioned on f being the first scheduled user and the feedback set being $\mathcal{B}_f$. From (8), the user scheduled on the downlink is the one in $\mathcal{B}_f$ that maximizes the downlink spectral efficiency. Therefore,

$$T_{\text{DL}}(f,\mathcal{B}_f) = \mathbb{E}\Bigg[\max_{i\in\mathcal{B}_f}\left\{\log_2\left(1+\hat{\gamma}_{\text{DL}}^{\text{FD}}(i)\right)\right\}|\mathcal{B}_f; \gamma_{\text{UL}}^{\text{FD}}(j) \le \gamma_{\text{UL}}^{\text{FD}}(f), \forall j \in \mathbb{N}\setminus\{f\}\Bigg]. \tag{44}$$

Since the downlink SINR of a user is independent of the uplink SINRs of the other users, (44) can be shown to simplify to

$$T_{\text{DL}}(f,\mathcal{B}_f) = \mathbb{E}\left[\max_{i\in\mathcal{B}_f}\left\{\log_2\left(1+\hat{\gamma}_{\text{DL}}^{\text{FD}}(i)\right)\right\}|\gamma_{\text{UL}}^{\text{FD}}(j) \le \gamma_{\text{UL}}^{\text{FD}}(f), \forall j \in \mathcal{B}_f\right]. \tag{45}$$

We know from (41) and (42) that $\gamma_{\text{UL}}^{\text{FD}}(f) \propto \max\{\alpha_f\} = \Theta(\log(N))$. Thus, $\gamma_{\text{UL}}^{\text{FD}}(f) \to \infty$ as $N \to \infty$ with probability 1. Since $|\mathcal{B}_f| \le L$, it follows that $\mathbb{P}\left(\gamma_{\text{UL}}^{\text{FD}}(j) \le \gamma_{\text{UL}}^{\text{FD}}(f), \forall j \in \mathcal{B}_f\right) \to 1$. Hence, the conditioning on the event $\gamma_{\text{UL}}^{\text{FD}}(j) \le \gamma_{\text{UL}}^{\text{FD}}(f), \forall j \in \mathcal{B}_f$, in (45) can be dropped:

$$T_{\text{DL}}(f,\mathcal{B}_f) = \mathbb{E}\left[\max_{i\in\mathcal{B}_f}\left\{\log_2\left(1+\hat{\gamma}_{\text{DL}}^{\text{FD}}(i)\right)\right\}\right]. \tag{46}$$

We now bound $T_{\text{DL}}(f,\mathcal{B}_f)$ on both sides.

i) Lower Bound: From the Jensen's inequality, we have $\mathbb{E}\left[\max_{i\in\mathcal{B}_f}\left\{\log_2\left(1+\hat{\gamma}_{\text{DL}}^{\text{FD}}(i)\right)\right\}\right] \ge \max_{i\in\mathcal{B}_f}\left\{\mathbb{E}\left[\log_2\left(1+\hat{\gamma}_{\text{DL}}^{\text{FD}}(i)\right)\right]\right\}$. Hence, from (12), it follows that

$$T_{\text{DL}}(f,\mathcal{B}_f) \ge \max_{i\in\mathcal{B}_f}\left\{\mathbb{E}\left[\log_2\left(1+\hat{\gamma}_{\text{DL}}^{\text{FD}}(i)\right)\right]\right\}. \tag{47}$$

Since $\log_2(1+e^x)$ is convex in x, Jensen's inequality implies that

$$T_{\text{DL}}(f,\mathcal{B}_f) \ge \max_{i\in\mathcal{B}_f}\left\{\log_2\left(1+\exp\left(\mathbb{E}\left[\log\left(\hat{\gamma}_{\text{DL}}^{\text{FD}}(i)\right)\right]\right)\right)\right\}. \tag{48}$$

Substituting (10) and simplifying, we get

$$T_{\text{DL}}(f,\mathcal{B}_f) \ge \max_{i\in\mathcal{B}_f}\left\{\log_2\left(1+\frac{P_{\text{BS}}\exp\left(\mathbb{E}\left[\log\left(h_i\right)\right]\right)}{\sigma_{\text{dl}}^2+\gamma_{\text{th}}}\right)\right\}. \tag{49}$$

From Lemma 1, $\gamma_{\text{th}} \to 0$. Furthermore, $\mathbb{E}[\log(h_i)] = \frac{1}{\mu'}\int_0^\infty \log(x)\exp\left(-\frac{x}{\mu'}\right)dx = \log(\mu') - E$. Hence, (49) reduces to

$$T_{\text{DL}}(f,\mathcal{B}_f) \ge \log_2\left(1+\frac{P_{\text{BS}}\mu'}{\sigma_{\text{dl}}^2}\exp(-E)\right). \tag{50}$$

ii) Upper Bound: We know that $\max_{i\in\mathcal{B}_f}\left\{\log_2\left(1+\hat{\gamma}_{\text{DL}}^{\text{FD}}(i)\right)\right\} \le \sum_{i\in\mathcal{B}_f}\log_2\left(1+\hat{\gamma}_{\text{DL}}^{\text{FD}}(i)\right)$. Also, from Lemma 1, $\mathbb{P}(|\mathcal{B}_f| = L) \to 1$. Substituting these in (46) and using the fact that $\hat{\gamma}_{\text{DL}}^{\text{FD}}(1), \hat{\gamma}_{\text{DL}}^{\text{FD}}(2), \ldots, \hat{\gamma}_{\text{DL}}^{\text{FD}}(N)$ are i.i.d., we get

$$T_{\text{DL}}(f,\mathcal{B}_f) \le L\mathbb{E}\left[\log_2\left(1+\hat{\gamma}_{\text{DL}}^{\text{FD}}(1)\right)\right]. \tag{51}$$

From [34, (36)], we have $\mathbb{E}\left[\log_2\left(1+\hat{\gamma}_{\text{DL}}^{\text{FD}}(i)\right)\right] \le \log_2(e)\exp\left(\frac{\sigma_{\text{dl}}^2}{P_{\text{BS}}\mu'}\right)\left[\frac{\sigma_{\text{dl}}^2}{P_{\text{BS}}\mu'} - \log\left(\frac{\sigma_{\text{dl}}^2}{P_{\text{BS}}\mu'}\right) - E\right]$. Therefore, we get

$$T_{\text{DL}}(f,\mathcal{B}_f) \le L\log_2(e)\exp\left(\frac{\sigma_{\text{dl}}^2}{P_{\text{BS}}\mu'}\right) \times \left[\frac{\sigma_{\text{dl}}^2}{P_{\text{BS}}\mu'} - \log\left(\frac{\sigma_{\text{dl}}^2}{P_{\text{BS}}\mu'}\right) - E\right]. \tag{52}$$

Combining (43)), (50), and (52) and using $\sum_{f\in\mathbb{N}}\sum_{\mathcal{B}_f}\mathbb{P}(f,\mathcal{B}_f) = 1$ yields (20).

2) Downlink First Case: We characterize the scaling behavior of C_{DL} and C_{UL} separately.

a) Scaling Behavior of C_{DL}: The downlink SINR γ_{DL} is given by $\gamma_{\text{DL}} = \max_{i\in\mathbb{N}}\left\{\hat{\gamma}_{\text{DL}}^{\text{FD}}(i)\right\}$. Substituting $\gamma_{\text{th}} \to 0$, $h_i = \alpha_i\mu'$, and (10) in this yields

$$\gamma_{\text{DL}} = \frac{P_{\text{BS}}\mu'}{\sigma_{\text{dl}}^2}\max_{i\in\mathbb{N}}\{\alpha_i\}. \tag{53}$$

Along lines similar to (41), we get $C_{\text{DL}} = \log_2\left(P_{\text{BS}}\mu'/\sigma_{\text{dl}}^2\right) + \log_2(\log(N)) + O(\log(\log(\log(N))))$.

b) Scaling Behavior of C_{UL}: The uplink user is scheduled second and chosen from the feedback set. Therefore, similar to (43), C_{UL} is given by

$$C_{\text{UL}} = \sum_{f\in\mathbb{N}}\sum_{\mathcal{B}_f}\mathbb{P}(f,\mathcal{B}_f)\,T_{\text{UL}}(f,\mathcal{B}_f), \tag{54}$$

where $T_{\text{UL}}(f,\mathcal{B}_f)$ is the average uplink spectral efficiency conditioned on user f being scheduled first and the feedback set being $\mathcal{B}_f$. In a manner similar to (46), we can show that $T_{\text{UL}}(f,\mathcal{B}_f) = \mathbb{E}\left[\max_{i\in\mathcal{B}_f}\left\{\log_2\left(1+\gamma_{\text{UL}}^{\text{FD}}(i)\right)\right\}\right]$. The above expectation is similar to (46), except that $\hat{\gamma}_{\text{DL}}^{\text{FD}}(i)$ is replaced by $\gamma_{\text{UL}}^{\text{FD}}(i)$. Therefore, as in the uplink first case, we get (22).

D. Proof of Lemma 2

Substituting (11) and the CDF $F_{g_{m,n}}(x) = 1 - Q\left(\left[\xi\log(x) - \tilde{\mu}''\right]/\tilde{\sigma}_{\text{dB}}\right)$, for $x \ge 0$, in (38), we get

$$\mathbb{P}(|\mathcal{B}_f| < L) = \sum_{\ell=0}^{L-1}\binom{N-1}{\ell}\left[1-Q\left(\frac{\xi}{\tilde{\sigma}_{\text{dB}}}\log\left(\frac{\gamma_{\text{th}}}{P_{\text{U}}}\right) - \frac{\tilde{\mu}''}{\tilde{\sigma}_{\text{dB}}}\right)\right]^{\ell} \times \left[Q\left(\frac{\xi}{\tilde{\sigma}_{\text{dB}}}\log\left(\frac{\gamma_{\text{th}}}{P_{\text{U}}}\right) - \frac{\tilde{\mu}''}{\tilde{\sigma}_{\text{dB}}}\right)\right]^{N-\ell-1}. \tag{55}$$

Let X_N be a binomial RV with parameter $p_N = 1 - Q\left(\frac{\xi}{\tilde{\sigma}_{\text{dB}}}\log\left(\frac{\gamma_{\text{th}}}{P_{\text{U}}}\right) - \frac{\tilde{\mu}''}{\tilde{\sigma}_{\text{dB}}}\right)$. As in Appendix B, when $N \to \infty$ and $p_N \to 0$, we get

$$\mathbb{P}(|\mathcal{B}_f| < L) = \mathbb{P}(X_N < L) \to 1 - Q\left(\frac{L-(N-1)p_N}{\sqrt{(N-1)p_N(1-p_N)}}\right). \tag{56}$$

For $\gamma_{\text{th}} = P_{\text{U}} \exp\left(\frac{\tilde{\mu}''}{\xi} - \frac{\zeta'\tilde{\sigma}_{\text{dB}}}{\xi}\sqrt{2\log(N)}\right)$ and $L \leq (N-1)^{\kappa'}\left[1 - Q\left(\zeta'\sqrt{2\log(N)}\right)\right]^{\kappa'}$, for any $0 < \zeta', \kappa' < 1$, the term inside the Q-function can be shown to converge to $-\infty$ and $\mathbb{P}(|\mathcal{B}_f| < L) \to 0$.

From (11), it follows that $\mathbb{P}(|\mathcal{B}_f| = 0) = \left(Q\left(\frac{\xi}{\tilde{\sigma}_{\text{dB}}}\log\left(\frac{\gamma_{\text{th}}}{P_{\text{U}}}\right) - \frac{\tilde{\mu}''}{\tilde{\sigma}_{\text{dB}}}\right)\right)^{N-1}$. Substituting $Q(x) = 1 - Q(-x)$ and $\gamma_{\text{th}} = P_{\text{U}} \exp\left(\frac{\tilde{\mu}''}{\xi} - \frac{\zeta'\tilde{\sigma}_{\text{dB}}}{\xi}\sqrt{2\log(N)}\right)$ in this expression and simplifying, we get

$$\mathbb{P}(|\mathcal{B}_f| = 0) = \left[1 - Q\left(\zeta'\sqrt{2\log(N)}\right)\right]^{N-1}. \quad (57)$$

Since $Q(x) \leq \exp\left(-\frac{x^2}{2}\right) / \left(\sqrt{2\pi}x\right)$ [35, Ch. 3.1], we get

$$\mathbb{P}(|\mathcal{B}_f| = 0) \geq \left(1 - \frac{1}{2\zeta' N^{\zeta'^2}\sqrt{\pi\log(N)}}\right)^{N-1} \to 1. \quad (58)$$

Therefore, $\mathbb{P}(|\mathcal{B}_f| = 0) \to 1$ for $\zeta' > 1$.

E. Brief Proof of Theorem 3

1) Uplink First Case: We first characterize the scaling behavior of C_{UL} and then C_{DL}.

a) Scaling Behavior of C_{UL}: Let

$$\Gamma_L \triangleq \frac{P_{\text{U}}}{\sigma_{\text{ul}}^2}\exp\left(\frac{\tilde{\mu}'}{\xi} + \frac{\tilde{\sigma}_{\text{dB}}}{\xi}\sqrt{2\left[\log(N) - \log(\log(N))\right]}\right), \quad (59)$$

$$\Gamma_U \triangleq \frac{P_{\text{U}}}{\sigma_{\text{ul}}^2}\exp\left(\frac{\tilde{\mu}'}{\xi} + \frac{\tilde{\sigma}_{\text{dB}}}{\xi}\sqrt{2\left[\log(N) + \log(\log(N))\right]}\right). \quad (60)$$

We shall show that $\mathbb{P}(\Gamma_L < \gamma_{\text{UL}} \leq \Gamma_U) \to 1$. Since both $\log_2(1+\Gamma_L)$ and $\log_2(1+\Gamma_U)$ scale as $\sqrt{\log(N)}$, so does C_{UL}. Specifically, from (59) and (60), we get $C_{\text{UL}} = \log_2\left(\frac{P_{\text{U}}}{\sigma_{\text{ul}}^2}\exp\left(\frac{\tilde{\mu}'}{\xi}\right)\right) + \frac{\tilde{\sigma}_{\text{dB}}}{\xi}\log_2(e)\sqrt{2\log(N)} + O(\log(\log(N)))$.

i) Evaluation of $\mathbb{P}(\gamma_{UL} > \Gamma_L)$: We have $F_{\gamma_{\text{UL}}^{\text{FD}}(i)}(x) = 1 - Q\left(\frac{\xi}{\tilde{\sigma}_{\text{dB}}}\log\left(\frac{\sigma_{\text{ul}}^2 x}{P_{\text{U}}}\right) - \frac{\tilde{\mu}'}{\tilde{\sigma}_{\text{dB}}}\right)$, for $x \geq 0$. Substituting this in $\mathbb{P}(\gamma_{\text{UL}} \leq \Gamma_L) = \prod_{i\in\mathbb{N}} F_{\gamma_{\text{UL}}^{\text{FD}}(i)}(\Gamma_L)$ and simplifying, we get

$$\mathbb{P}(\gamma_{\text{UL}} \leq \Gamma_L) = \left[1 - Q\left(\sqrt{2\left[\log(N) - \log(\log(N))\right]}\right)\right]^N. \quad (61)$$

Since $Q(x) \geq \frac{1}{\sqrt{2\pi}x}\left(1 - \frac{1}{x^2}\right)\exp\left(-\frac{x^2}{2}\right)$ [35, Ch. 3.1], we get

$$\begin{aligned}\mathbb{P}(\gamma_{\text{UL}} \leq \Gamma_L) &\leq \left[1 - \frac{\log(N)\left(1 - \left[2\left(\log(N) - \log(\log(N))\right)\right]^{-1}\right)}{2N\sqrt{\pi\left[\log(N) - \log(\log(N))\right]}}\right]^N, \\ &\leq \exp\left(-\frac{\log(N)\left(1 - \left[2\left(\log(N) - \log(\log(N))\right)\right]^{-1}\right)}{2\sqrt{\pi\left[\log(N) - \log(\log(N))\right]}}\right). \end{aligned} \quad (62)$$

It can be shown that the term inside the exponential function converges to $-\frac{1}{2\sqrt{\pi}}\sqrt{\log(N)} = -\infty$. Therefore, $\mathbb{P}(\gamma_{\text{UL}} \leq \Gamma_L) \to 0$. Hence, $\mathbb{P}(\gamma_{\text{UL}} > \Gamma_L) \to 1$.

ii) Evaluation of $\mathbb{P}(\gamma_{UL} < \Gamma_U)$: Along similar lines, we can show that $\mathbb{P}(\gamma_{\text{UL}} < \Gamma_U) \to 1$.

b) Scaling Behavior of C_{DL}: Similar to Appendix C, we first bound $T_{\text{DL}}(f, \mathcal{B}_f)$.

i) Lower Bound: Substituting $\gamma_{\text{th}} \to 0$ (from Lemma 2) and $\mathbb{E}[\log(h_i)] = \tilde{\mu}'/\xi$ in (49) yields

$$T_{\text{DL}}(f, \mathcal{B}_f) \geq \log_2\left(1 + \frac{P_{\text{BS}}}{\sigma_{\text{dl}}^2}\exp\left(\frac{\tilde{\mu}'}{\xi}\right)\right). \quad (63)$$

Substituting (63) in (43) yields the lower bound in (25).

ii) Upper Bound: Substituting $\gamma_{\text{th}} \to 0$ and (10) in (51), we get

$$\begin{aligned} T_{\text{DL}}(f, \mathcal{B}_f) &\leq L\mathbb{E}\left[\log_2\left(1 + \tfrac{P_{\text{BS}}h_i}{\sigma_{\text{dl}}^2}\right)\right], \\ &\leq L\log_2\left(1 + \tfrac{P_{\text{BS}}}{\sigma_{\text{dl}}^2}\mathbb{E}[h_i]\right). \end{aligned} \quad (64)$$

Substituting $\mathbb{E}[h_i] = \exp\left(\frac{\tilde{\mu}'}{\xi} + \frac{\tilde{\sigma}_{\text{dB}}^2}{2\xi^2}\right)$, we get

$$T_{\text{DL}}(f, \mathcal{B}_f) \leq L\log_2\left(1 + \frac{P_{\text{BS}}}{\sigma_{\text{dl}}^2}\exp\left(\frac{\tilde{\mu}'}{\xi} + \frac{\tilde{\sigma}_{\text{dB}}^2}{2\xi^2}\right)\right). \quad (65)$$

Substituting (65) in (43) yields the upper bound in (25).

2) Downlink First Case: The analysis of the scaling behavior of C_{UL} is similar to that for C_{DL} above, and that for C_{DL} is similar to that for C_{UL} above. We skip them to conserve space.

REFERENCES

[1] R. Kiran and N. B. Mehta, "Reduced feedback, user scheduling, and mode selection in asymmetric full-duplex systems," in *Proc. IEEE Global Commun. Conf. (GLOBECOM)*, Dec. 2020, pp. 1–6.

[2] K. E. Kolodziej, B. T. Perry, and J. S. Herd, "In-band full-duplex technology: Techniques and systems survey," *IEEE Trans. Microw. Theory Techn.*, vol. 67, no. 7, pp. 3025–3041, Jul. 2019.

[3] S. Shao, D. Liu, K. Deng, Z. Pan, and Y. Tang, "Analysis of carrier utilization in full-duplex cellular networks by dividing the co-channel interference region," *IEEE Commun. Lett.*, vol. 18, no. 6, pp. 1043–1046, Jun. 2014.

[4] Z. Liu, Y. Liu, and F. Liu, "Joint resource scheduling for full-duplex cellular system," in *Proc. 22nd Int. Conf. Telecommun. (ICT)*, Apr. 2015, pp. 85–90.

[5] B. Li, C. Li, C. Yang, and B. Xia, "User scheduling for full-duplex cellular networks," in *Proc. IEEE Int. Conf. Commun. Workshops (ICC Workshops)*, May 2019, pp. 1–6.

[6] J. Zhao, S. Han, C. Yang, Y. Teng, and N. Zheng, "Location-based bidirectional user scheduling and mode selection in full-duplex system," in *Proc. IEEE Global Conf. Signal Inf. Process. (GlobalSIP)*, Dec. 2016, pp. 679–683.

[7] G. C. Alexandropoulos, M. Kountouris, and I. Atzeni, "User scheduling and optimal power allocation for full-duplex cellular networks," in *Proc. IEEE 17th Int. Workshop Signal Process. Adv. Wireless Commun. (SPAWC)*, Jul. 2016, pp. 1–6.

[8] D. Wen and G. Yu, "Time-division cellular networks with full-duplex base stations," *IEEE Commun. Lett.*, vol. 20, no. 2, pp. 392–395, Feb. 2016.

[9] H.-H. Choi, "On the design of user pairing algorithms in full duplexing wireless cellular networks," in *Proc. Int. Conf. Inf. Commun. Technol. Converg. (ICTC)*, Oct. 2014, pp. 490–495.

[10] C. Nam, C. Joo, S.-G. Yoon, and S. Bahk, "Resource allocation in full-duplex OFDMA networks: Approaches for full and limited CSIs," *J. Commun. Netw.*, vol. 18, no. 6, pp. 913–925, Dec. 2016.

[11] B. Di, S. Bayat, L. Song, Y. Li, and Z. Han, "Joint user pairing, subchannel, and power allocation in full-duplex multi-user OFDMA networks," *IEEE Trans. Wireless Commun.*, vol. 15, no. 12, pp. 8260–8272, Dec. 2016.

[12] M. Feng, S. Mao, and T. Jiang, "Duplex mode selection and channel allocation for full-duplex cognitive femtocell networks," in *Proc. IEEE Wireless Commun. Netw. Conf. (WCNC)*, Mar. 2015, pp. 1900–1905.

[13] R. Sultan, L. Song, K. G. Seddik, and Z. Han, "Joint resource management with distributed uplink power control in full-duplex OFDMA networks," *IEEE Trans. Veh. Technol.*, vol. 69, no. 3, pp. 2850–2863, Mar. 2020.
[14] L. Chen, C. Zhong, H. Lin, and Z. Zhang, "Joint user pairing and power allocation design for heavy loaded full-duplex small cell systems," *IEEE Trans. Veh. Technol.*, vol. 67, no. 9, pp. 8989–8993, Sep. 2018.
[15] C.-C. Chao, C.-Y. Wang, C.-H. Lee, H.-Y. Wei, and W.-T. Chen, "Pair auction and matching for resource allocation in full-duplex cellular systems," *IEEE Trans. Veh. Technol.*, vol. 69, no. 4, pp. 4325–4339, Apr. 2020.
[16] Y.-Y. Chang and H.-J. Su, "Distributed user pairing and transmission mode selection in a single cell full duplex network," in *Proc. IEEE 90th Veh. Technol. Conf. (VTC-Fall)*, Sep. 2019, pp. 1–5.
[17] J. M. B. da Silva, G. Fodor, and C. Fischione, "Fast-Lipschitz power control and user-frequency assignment in full-duplex cellular networks," *IEEE Trans. Wireless Commun.*, vol. 16, no. 10, pp. 6672–6687, Oct. 2017.
[18] J. M. B. da Silva, G. Fodor, and C. Fischione, "On the spectral efficiency and fairness in full-duplex cellular networks," in *Proc. IEEE Int. Conf. Commun. (ICC)*, May 2017, pp. 1–6.
[19] X. Zhang, T. H. Chang, Y. F. Liu, C. Shen, and G. Zhu, "Max-min fairness user scheduling and power allocation in full-duplex OFDMA systems," *IEEE Trans. Wireless Commun.*, vol. 18, no. 6, pp. 3078–3091, Jun. 2019.
[20] J. M. B. da Silva, G. Fodor, and C. Fischione, "Spectral efficient and fair user pairing for full-duplex communication in cellular networks," *IEEE Trans. Wireless Commun.*, vol. 15, no. 11, pp. 7578–7593, Nov. 2016.
[21] X. Shen, X. Cheng, L. Yang, M. Ma, and B. Jiao, "On the design of the scheduling algorithm for the full duplexing wireless cellular network," in *Proc. IEEE Global Commun. Conf. (GLOBECOM)*, Dec. 2013, pp. 4970–4975.
[22] A. C. Cirik, K. Rikkinen, and M. Latva-aho, "Joint subcarrier and power allocation for sum-rate maximization in OFDMA full-duplex systems," in *Proc. IEEE 81st Veh. Technol. Conf. (VTC Spring)*, May 2015, pp. 1–5.
[23] M. Al-Imari, M. Ghoraishi, P. Xiao, and R. Tafazolli, "Game theory based radio resource allocation for full-duplex systems," in *Proc. IEEE 81st Veh. Technol. Conf. (VTC Spring)*, May 2015, pp. 1–5.
[24] P. Tehrani, F. Lahouti, and M. Zorzi, "Resource allocation in OFDMA networks with half-duplex and imperfect full-duplex users," in *Proc. IEEE Int. Conf. Commun. (ICC)*, May 2016, pp. 1–6.
[25] A. C. Cirik, K. Rikkinen, R. Wang, and Y. Hua, "Resource allocation in full-duplex OFDMA systems with partial channel state information," in *Proc. IEEE China Summit Int. Conf. Signal Inf. Process. (ChinaSIP)*, Jul. 2015, pp. 711–715.
[26] Y. Yang, C. Nam, and N. B. Shroff, "A near-optimal randomized algorithm for uplink resource allocation in OFDMA systems," in *Proc. 12th Int. Symp. Model. Optim. Mobile, Ad Hoc, Wireless Netw. (WiOpt)*, May 2014, pp. 218–224.
[27] M. S. Elbamby, M. Bennis, W. Saad, M. Debbah, and M. Latva-Aho, "Resource optimization and power allocation in in-band full duplex-enabled non-orthogonal multiple access networks," *IEEE J. Sel. Areas Commun.*, vol. 35, no. 12, pp. 2860–2873, Dec. 2017.
[28] M. Abramowitz and I. Stegun, *Handbook of Mathematical Functions, With Formulas, Graphs, and Mathematical Tables*, 9th ed. New York, NY, USA: Dover, 1972.
[29] J. Kleinberg and E. Tardos, *Algorithm Design*, 14th ed. London, U.K.: Pearson Education, 2013.
[30] E. Kreyszig, *Advanced Engineering Mathematics*, 10th ed. Hoboken, NJ, USA: Wiley, 2010.
[31] M. Sharif and B. Hassibi, "On the capacity of MIMO broadcast channels with partial side information," *IEEE Trans. Inf. Theory*, vol. 51, no. 2, pp. 506–522, Feb. 2005.
[32] N. Mehta, J. Wu, A. Molisch, and J. Zhang, "Approximating a sum of random variables with a lognormal," *IEEE Trans. Wireless Commun.*, vol. 6, no. 7, pp. 2690–2699, Jul. 2007.
[33] A. Papoulis, *Probability, Random Variables, and Stochastic Processes*, 3rd ed. New York, NY, USA: McGraw-Hill, 1991.
[34] M.-S. Alouini and A. J. Goldsmith, "Capacity of Rayleigh fading channels under different adaptive transmission and diversity-combining techniques," *IEEE Trans. Veh. Technol.*, vol. 48, no. 4, pp. 1165–1181, Jul. 1999.
[35] U. Madhow, *Fundamentals of Digital Communication*, 1st ed. Cambridge, U.K.: Cambridge Univ. Press, 2008.

Rama Kiran received the B.E. degree in telecommunication engineering from the PES Institute of Technology, Bengaluru, India, in 2011, and the M.Tech. degree in electrical engineering from the Indian Institute of Technology (IIT) Kanpur in 2014. He is currently pursuing the Ph.D. degree with the Department of Electrical Communication Engineering, Indian Institute of Science (IISc), Bengaluru. From 2014 to 2015, he was with NI Systems (India) Pvt., Ltd., Bengaluru, where he worked on the development and implementation of algorithms for LTE and IEEE 802.11b/af/ah wireless standards. His research interests include wireless communication, full-duplex communication, and next generation wireless standards.

Neelesh B. Mehta (Fellow, IEEE) received the B.Tech. degree in electronics and communications engineering from the Indian Institute of Technology (IIT) Madras in 1996, and the M.S. and Ph.D. degrees in electrical engineering from the California Institute of Technology, Pasadena, USA, in 1997 and 2001, respectively. He is currently a Professor with the Department of Electrical Communication Engineering, Indian Institute of Science, Bengaluru. He is a fellow of the Indian National Science Academy (INSA), the Indian National Academy of Engineering (INAE), and the National Academy of Sciences India (NASI). He was a recipient of the Shanti Swarup Bhatnagar Award, the Khosla Award, the Vikram Sarabhai Research Award, and the Swarnjayanti Fellowship. He served on the Board of Governors for the IEEE ComSoc from 2012 to 2015. He served on the Executive Editorial Committee for IEEE TRANSACTIONS ON WIRELESS COMMUNICATIONS from 2014 to 2017, and served as its Chair from 2017 to 2018. He has served as an Editor for the IEEE TRANSACTIONS ON COMMUNICATIONS and the IEEE WIRELESS COMMUNICATION LETTERS in the past.